NanoTodaylpQpijZ^^lftjop, Qnly.

Contents lists available at ScienceDirect

Nano Today

journal homepage: www.elsevier.com/locate/nanotoday

Review

Covalent three-dimensional networks of graphene and carbon nanotubes: synthesis and environmental applications

Archi Dasgupta[a], Lakshmy Pulickal Rajukumar[b], Christopher Rotella[b], Yu Lei[b], Mauricio Terrones[a,b,c,*]

[a] Department of Chemistry, The Pennsylvania State University, University Park, PA 16802, USA
[b] Department of Materials Science and Engineering, The Pennsylvania State University, University Park, PA 16802, USA
[c] Department ofPhysics and Center for2-Dimensional and Layered Materials, The Pennsylvania State University, University Park, PA 16802, USA

ARTICLE INFO

Article history:
Received 8 October 2016 Received in revised form 21 November 2016
Accepted 10 December 2016 Available online 28 December 2016

Keywords:
Three-dimensional networks
Carbon nanotubes
Graphene
Hybrid structures
Properties
Adsorption
Pollution management

ABSTRACT

In recent years tremendous efforts have been made to exploit the exceptional properties of 1-Dimensional
carbon nanotubes and 2-Dimensional graphene in order to interconnect those forming 3-Dimensional
hybrid systems. Such macroscopic 3-D networks possess several advantages such as highly accessible
surface area, minimized agglomeration or re-stacking, enhanced thermal and electrical transport, and
robust mechanical properties as compared to their nanoscale 1-D or 2-D building blocks. This review
aims to provide a fundamental understanding of state of the art synthesis methodologies for

Contents

* Corresponding author at: Department of Chemistry, The Pennsylvania State University, University Park, PA 16802, USA. *E-mail address:* mut11@psu.edu (M. Terrones).

http://dx.doi.org/10.1016/j.nantod.2016.12.011
1748-0132/

Introduction

Assembling nanostructures to fabricate macroscopic materials for practical applications is a continuing challenge in modern nanotechnology. Theoretical predictions have indicated that if carbon nanostructures such as 1-dimensional carbon nanotubes (CNTs) or 2-dimensional graphene are assembled into 3-dimensional macrostructures, unprecedented mechanical, electronic and sur- face characteristics can be achieved [1-3]. Fig. 1 demonstrates various spatial arrangements of sp^2 hybridized carbon atoms that could be used as building blocks to construct 3-D hybrid networks.

To achieve the above mentioned assemblies, the very initial approaches consisted of merging single and double walled CNTs (SWNTs and DWNTs) covalently, using electron beam exposure at high temperatures [4], or by incorporating atomic welders (e.g. Boron) during thermal annealing [5] (Fig. 2a and b). By extrapolating this concept, various models of interconnected CNTs [3], graphene sheets [6], graphene-CNT hybrids [6] and fullerene-CNT hybrids [7] have been proposed.The energeticstability, mechanical, electronic transport, and porosity properties of 3-D superlattices (namely "SuperDiamond", SD and "SuperCubic", SC structures) constructed from CNTs were proposed and studied by Romo-Herrera et al. [3] (Fig. 2c and d). Non hexagonal carbon rings such as pentagons, heptagons and octagons were employed to covalently interconnect the CNTs at multi terminal nodes and hierarchical structures were created. Owing to strong covalent interconnections between individual CNTs, the mechanical strength of these materials for axial compression was found to surpass that of their building blocks. The SD and SC networks were able to support a reduction of ~50% and ~30% of the initial length along the [001] direction compared to ~7% for CNTs. Additionally, depend- ing on the node-node lengths, van der Waals surface areas up to 2775 m^2g^{-1} and densities as low as 0.009 g cm^{-3} were calculated for these 3-D systems. Their remarkable electronic and mechanical properties, large surface area and porosity make these structures excellent candidates for fabricating novel catalysts, sensors, fil ters, and molecular storage materials. Dimitrakakis et al. studied hydrogen storage in 3-D graphene/CNT networks with tunable pore size and surface areas using *ab initio* and grand canonical Monte Carlo (GCMC) calculations [6]. The proposed novel 3-D material consisted of parallel graphene layers at a variable dis- tance, stabilized by CNTs placed vertically to the graphene planes. Hydrogen's interactions were calculated for heptagons (site A), the lower hexagons (site B) and the upper hexagons (site C) (Fig. 2e and f). It was shown that heptagonal rings were more favorable than the hexagonal ones regarding H_2 interaction at the junc- tion of the pillared tubes. Moreover, this material, when doped with lithium cations, could store up to 41 g H_2/L under ambient conditions, almost reaching DoE (United States 'Department of Energy') volumetric requirement (45 g H_2/L) for mobile applica- tions [6].

Since 2010 assembly of graphene and CNTs into 3-D architectures have been one of the most investigated areas of nanotechnology research. The integrated morphology of 3-D networks provides superior properties as compared to their building blocks, as it prevents aggregation and re-stacking, which are limiting factors in practical utilization of CNTs and graphene. Moreover, the highly interconnected structures and porosity of these materials result in accessibility of the internal surface area and facile mass transport. These unique properties coupled with inherent hydrophobicity, conductivity, and stability of CNTs and graphene provide a great platform for disposal and detection of diverse pollutants. Although synthesis and applications of 3-D graphene/CNT architectures have been reviewed in the past [8-10], the rapid research growth in this area prompted us to summarize the latest synthesis method, structure-property relationships and recently reported environmental applications. This review aims to provide a criti- cal understanding of the research concerning 3-D graphene/CNT solids from both a theoretical and technical point of view, as well as to shed light on current challenges and future opportuni- ties.

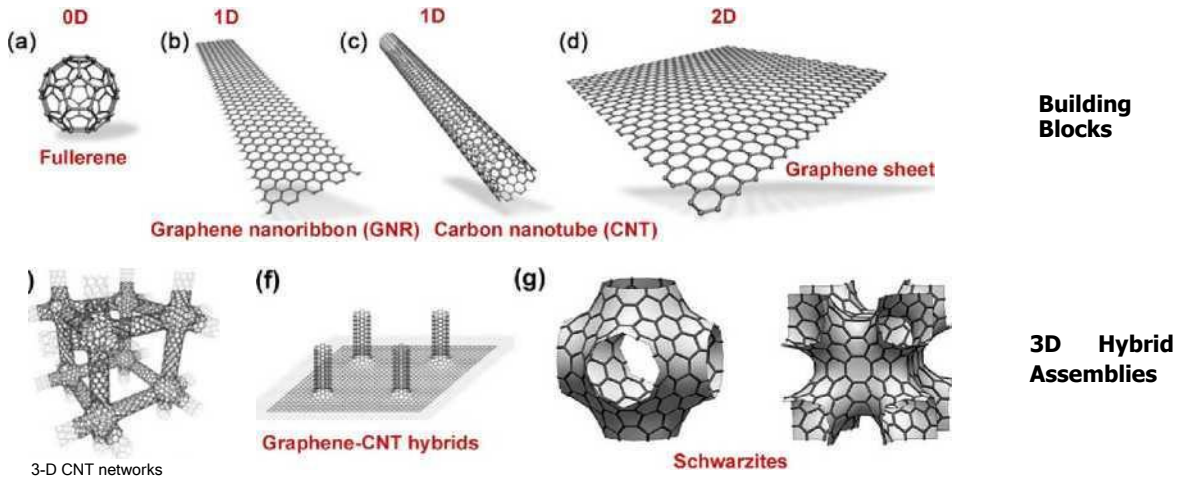

Fig. 1. Molecular models ofsp^2 hybridized carbon building blocks and the resulting3D hybrid assemblies. (a) Fullerene (0D); (b) Graphene nanoribbon(GNR)(1D); (c) Carbon nanotube (1D); (d) Graphene sheet (2D); (e) 3D CNT networks (3D); (f) Hybrid ofgraphene with CNTs (3D); (g) Graphene triple periodical minimal surfaces (orSchwarzites -3Dgraphene) showing non hexagonal rings such as heptagons oroctagons.

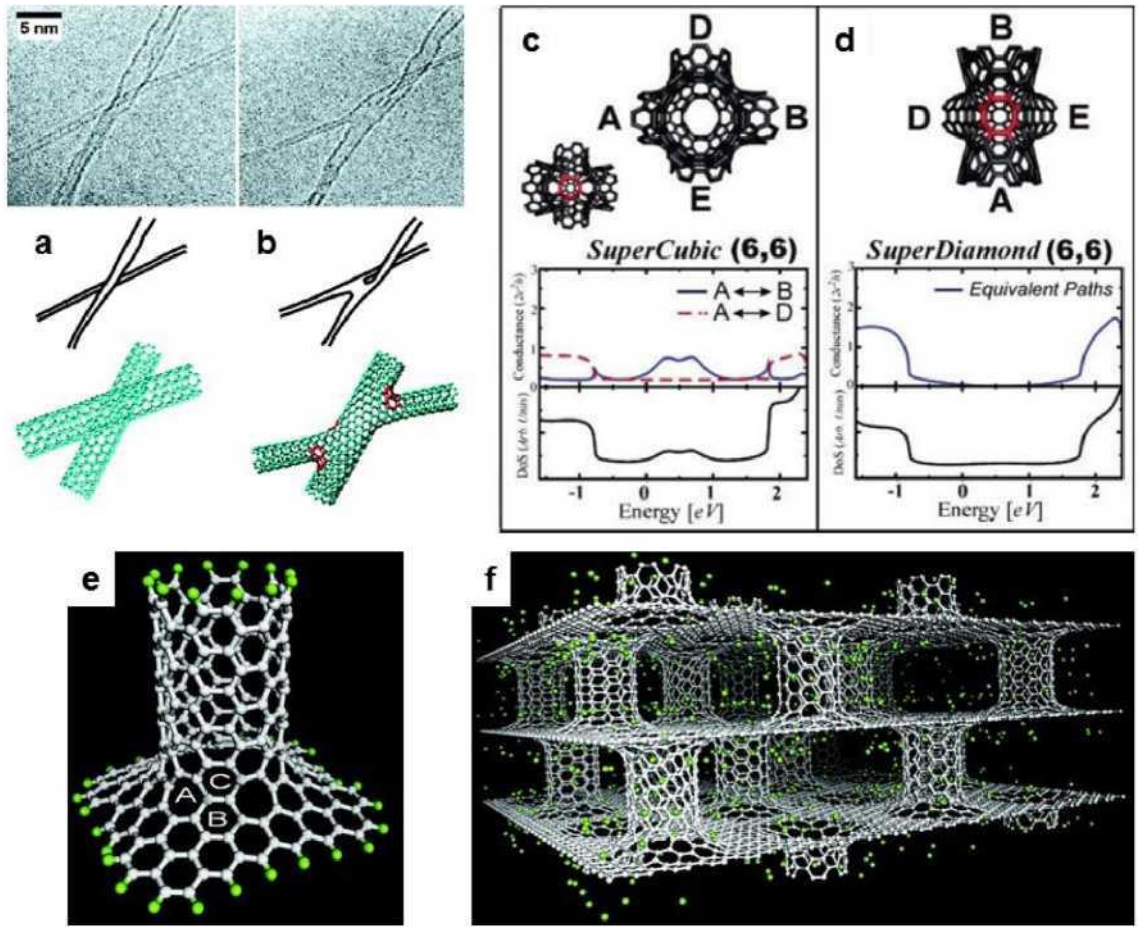

Fig. 2. (a) Two individual SWNTs Crossing each other. (b) Junction formation between the Crossing tubes by 60 s of electron irradiation [4]. Reprinted with permission from reference 4. Copyright 2002 American Physical Society; (c)and(d) The architecture, electrical conductivities and density of states (DoS) along different conduction pathways of Supercubic and Superdiamond structures [3]. X-axes show Energy [Ev] and Y axes in the bottom plots and top plots show DoS (Arb. Units.) and Conductance ($2e^2/h$) respectively. Reprinted with permission from reference 3. Copyright 2007 American Chemical Society; (e) Optimized cluster of a (6,6) CNT and graphene sheet; the beginning of the 3-D network nanostructure. Hydrogen's interaction was examined on the heptagon (site A), the lower hexagon (site B), and the upper hexagon (siteC). (f) Snapshot from the GCMC simulations of pure pillared structure at 77 K and 3 bar. Hydrogen molecules are represented in green (6). Reprinted with permission from reference 6. Copyright 2008 American Chemical Society. (For interpretation of the references to colour in this figure legend, the reader is referred to the web version of this article.)

Synthesis of graphene-based three dimensional structures

The exceptional mechanical and electrical properties of graphene (an atom thick sp^2 hybridized carbon layer), make it extremely attractive for numerous applications. However, its chemical inertness hinders its controlled assembly into 3- dimensional networks. Therefore, functionalization or oxidation of graphene monolayers are necessary. In this context, graphene oxide (GO), consisting of oxidized layered sheets of graphene with facile water solubility, but with less favorable electrical properties, can been synthesized chemically by the Hummers' method [11] using bulk graphite as a precursor. To improve its electrical properties, further reduction of GO by chemical or thermal routes is possible. This reduction, however, limits the mechanical capabilities of the material, creating a trade-off between GO and reduced graphene oxide (rGO) [12]. Novel methods that are currently being explored to create three-dimensional structures of graphene, GO and rGO will be discussed in the following sections.

Three dimensional graphene monoliths obtained from GO suspensions

Studies on graphene and GO foams synthesized from GO suspensions have been recently published [13-20]. For example, the colloidal properties of GO facilitate their assembly in order to form 3-D architectures. The striking features of GO, in addition to being densely decorated with carboxyl, epoxy and hydroxyl groups (Fig. 3a), are the forces of interaction between the layers. These forces are electrostatic as well as van der Waals in nature. Var- ious external agents have been used to manipulate these forces by changing the chemical environment of GO. Thus, cross-linking or gelation of the GO layers can be easily achieved and has been demonstrated by various routes. Shi et al. were one of the first groups to demonstrate the cross-linking of GO using poly vinyl alco- hol (PVA) [13]. These authors were able to obtain a pH sensitive, viscous hydrogel of GO and PVA on mixing various concentrations of both constituents. These hydrogels showed reversible sol-gel transformations depending on the pH. Fig. 3b shows the concen- tration ratio dependence of the cross-linker PVA to GO that were found to be effective for gelation and hydrogel formation [13].

Other agents that have successfully demonstrated the gela- tion of GO are: polymers such as hydroxypropylcellulose (HPC), poly(ethylene oxide) (PEO), and poly(vinyl pyrrolidone) (PVP), multivalent cations, biological molecules such as DNA, quaternary ammonium salts and amino acids [14,15]. The interaction between the GO layers has also been linked to their lateral dimensions and the distance between the layers [14]. Thus, Nguyen et al. conducted a study in this regard and tried and break down the layers into

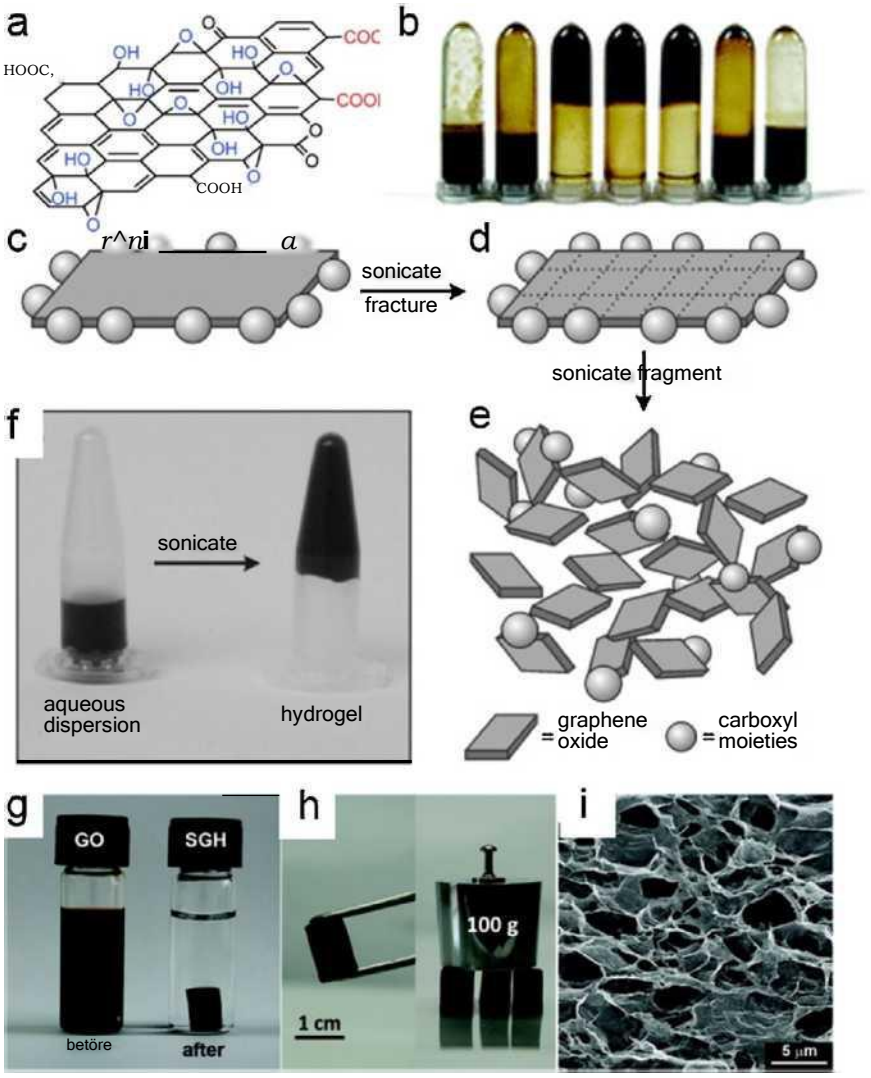

Fig. 3. (a) An Illustration of a layer of GO showing the attachment of —OH and —COOH groups to the honey comb shaped hexagonal carbon lattice [14]. Reprinted with permission from reference 14. Copyright 2011 American Chemical Society; (b) Different concentrations of a cross-linker PVA mixed with a GO solution showing the effect of PVA:GO ratio ($r_{P/G}$). From left to right, the ratios are: 1:1,1:1.5,1:2,1:5,1:10,1:20,1:40. The optimum concentration ofthe cross-linker to GO is found to be between 1:2 and 1:10 for effective gelation [13]. Reprinted with permission from reference 13. Copyright 2010 Royal Society of Chemistry; (c)-(e) Schematic of the ultrasonication process of fragmenting the GO layers into smaller domains, thus reducing the number of —COOH groups on the newly formed edges. (f) The aqueous dispersion of GO converted to a hydrogel afterthe ultrasonication [16]. Reprinted with permission from reference 16. Copyright 2012 Elsevier Ltd.; (g) Self-assembled graphene hydrogel (SGH) formed from a GO dispersion after a one-step hydrothermal process at 180 °C for 12 h. (h) Demonstration ofthese SGH supporting weights (100 g). (i) Internal pore structure ofSGH showing an interconnected network of graphene layers [17]. Reprinted with permission from reference 17. Copyright 2010 American Chemical Society.

smaller domains, using mechanical agitation with a probe sonica- tor [16]. A schematic scheme of their process is shown in Fig. 3(c-e). The authors were able to initiate gelation in the sonicated GO suspension (Fig. 3f) because of the formation of newly exposed layers of GO with reduced functional moieties, that decrease the stabil- ity of the dispersion [16]. The reduction of GO suspensions is an alternative approach to create cross-links among layers. A single step hydrothermal process to synthesize crosslinked hydrogels of GO was reported in 2010 [17]. This was a simple, yet efficient and reproducible route that involved the heating of an aqueous disper- sion of GO in an autoclave at 180°C for 12h. This process yielded free standing monolithic hydrogels of reduced GO. The conver- sion of GO into a self-assembled graphene hydrogel (SGH) after the hydrothermal process, is shown in Fig. 3g. Three SGH columns with a diameter around 0.8 cm each could support weights up to 100 g (Fig. 3h). Interestingly, the microstructure of these materials reveal an intricate well connected pore structure, which is supported by a cross-linked 3-D graphene network as shown in Fig. 3i. Many sub- sequent variations of this technique have been reported, such as replacing water with organic solvents such as ethanol (Fig. 4a-d) [18]. Reducing agents such as ethylenediamine (EDA), hydrazine, and ascorbic acid have also been found to be effective for creating stable gels of GO [19-21].

The drying of cross-linked GO gels is an important step in deter- mining the final pore structure of resulting 3-D solids. Some of the drying techniques that have been employed to create aerogels are: freeze-drying, super critical drying, vacuum drying, freeze casting, and heat drying [22-26]. Freeze drying is the most popular among all the drying techniques, and is carried out with hydrogels of GO. Solvent exchange with water is necessary as a preliminary step to freeze drying if organic solvents are used during the gelation process [18]. Shi et al. recently reported a new strategy for an effec- tive hydrothermal reduction of GO, which involved mixing of an aqueous GO suspension with hexane to form an emulsion [27]. The emulsion was then heated, in a Teflon-lined autoclave, to 180 °C for 10 h, which allowed the GO to be hydrothermally reduced. Upon

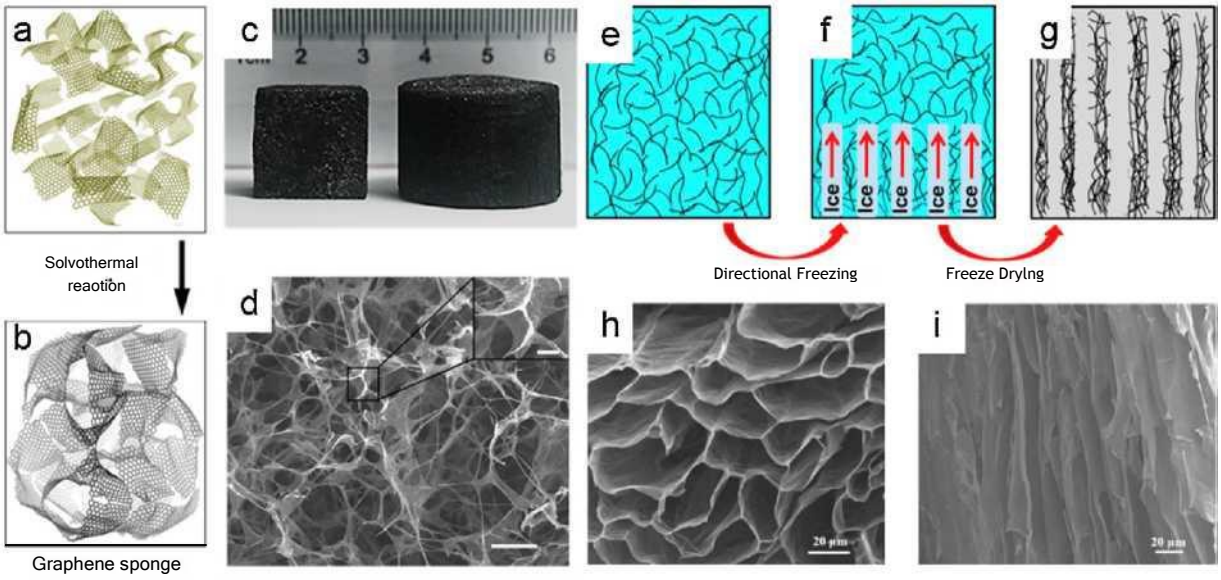

Fig. 4. (a) and (b) An Illustration of the solvothermal synthesis method to obtain cross-linked graphene layers from a GO dispersion in ethanol. (c) Free-standing blocks of interconnected graphene sponges in square and cylindrical shapes after freeze-drying the solvent exchanged hydrogels. (d) Microstructure of the 3-D graphene aerogels showing three-dimensionally bonded graphene layers (scalebar 20|xm) and a magnified SEM image (inset, scale bar 5 |xm) [18]. Reprinted with permission from reference 18. Copyright 2015 Nature Publishing Group; (e)-(g) A schematic outline ofthe directional freezing process used forchanneling the ice crystallization in a graphene aqueous solution. This results in the assembly of graphene layers around the ice channels. On freeze-drying, a graphene aerogel with highly uni-directional pores is left behind. (h) and (i) The micro-structure of directionally frozen graphene aerogels showing the uni-directional pore structure (scale bar, 20 |xm) [28]. Reprinted with permission from reference 28. Copyright 2016 Elsevier Ltd.

hexane evaporation, a hydrogel of rGO was obtained, which was subjected to a fast freezing process by immersing it first in liquid nitrogen. During the drying, ice crystals formed during the freezing step were sublimed directly into the gas phase, thus leaving behind a monolithic 3-D graphene aerogel. The concentration of the GO in the gel also plays a major role in determining the pore structure of the aerogel. It is necessary to surpass the percolation threshold in order to form a 3-dimensional interconnected pore structure. Another drying approach, super critical drying, typically involves 2 steps: 1) A solvent exchange in which liquid CO_2 occupies the pores of the gel, followed by 2) A drying step, which is carried out at temperatures and pressure conditions above the critical values of CO_2 (304.25 K, 72.9 atm) [26]. Freeze casting - yet another drying technique - was adopted by Li et al. to obtain 3-D aerogels of graphene with exceptional mechanical stability and hierarchi- cal structure comparable to that of cork [24]. This technique relies on the liquid-particle and particle-particle interactions when ice crystals form when freezing the GO gel. In this technique, a tem- perature gradient spurred a directional growth of ice crystals, thus trapping the GO layers between the crystals. A schematic of this process is shown in Fig. 4e-g. Upon removal of ice by sublimation, a macro-porous material was left behind, with a uni-directional pore structure (Fig. 4h and i) [28]. This type of directional freezing approach has also been adopted by Yu et al. to fabricate anisotropic graphene aerogels (AGAs) that showed superior absorption capac- ities (~200 times more than its own weight) for organic solvents, with a strikingly high absorption rate ($40gg^{-1}\ s^{-1}$) [28].

Recently, base-induced liquid crystals (LCs) of GO have been employed for creating long-range organization of graphene sheets in resulting 3-D foams [29]. Using normal-sized GO sheets (<10 |am), the formation of nematic LC phase usually requires a high GO concentration ($10mgmL^{-1}$) [30]. In this work, Yao et al. [29] demonstrated that strong bases such as KOH can induce the forma- tion of highly oriented LC at a low GO concentration (3.5 mg mL^{-1}). The orientation of GO sheets in LC was retained in the 3-D foams obtained after hydrothermal reduction of the LC and subsequent freeze drying. This work provides a new methodology to regulate self-assembly of GO sheets for the formation of ultralight, highly ordered GO foams.

Template directed approaches

Using sacrificial templates is an emerging alternative to create 3-D assemblies of graphene and GO [31-35]. Chen et al. demonstrated the use of porous nickel scaffolds to grow 3-D graphene foams after methane vapor deposition [32]. The advantage of this technique is that the Ni scaffold can be easily removed by etching it away using hydrochloric acid, thus leaving behind a monolithic freestanding 3-D graphene foam or sponge. The versatility of the template-based approach lies in the number of different templates that are available for growing different 3-D structures. Fig. 5a-d shows a schematic of controllably assembling a 3-D Ni scaffold using electrodeposi- tion and photolithography, to obtain a 3-D graphene system during chemical vapor deposition (CVD). After etching away the Ni scaffold, the micro structure of the resulting self-standing 3-D graphene structure is shown in Fig. 5e and f. Mesoporous mixed metal oxide templates with hierarchical pores, have also been tested as hard templates for growing 3-D graphene structures (see Fig. 5g) [36]. Recently, hydrophobic graphene foams with high sorption capaci- ties for oil and organic solvents (>200 gg^{-1}) were synthesized using a simple hard-template method reported by Du et al. [37] In this method, 3-D porous polyurethane (PU) sponges, were dipped in GO solution and burnt in air for less than a minute. The burning process removed the template and at the same time incorporated nitrogen atoms into the resulting porous graphene structure so as to yield N-doped graphene foams. The N-doping resulted in higher capac- itive performance than conventional graphene foams prepared by CVD on nickel foam templates [37].

Soft and hard templates have also been used to fabricate graphene-based porous 3-D structures through solution processing routes. In this context, Huh et al., used pH control and a filtration technique to obtain films consisting of GO colloidal particles and polystyrene (PS) micro spheres from their dispersions [39]. The PS particles were then selectively removed using toluene, leaving

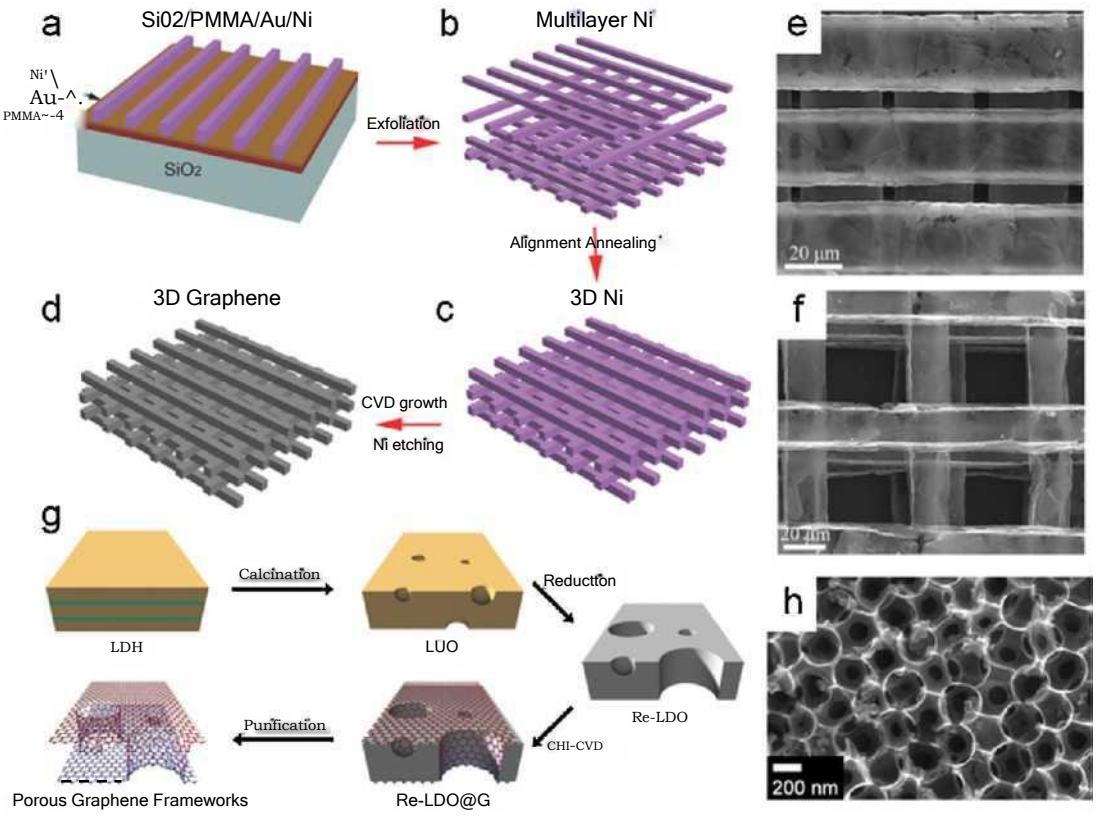

Fig. 5. (a)-(d) Ascheme illustratingthe layer-by-layerassembly ofa3-D Ni scaffold andsubjecting it toaCVD process forgrowing graphene overthe Ni. Ni etching yieldsself- standing 3-D graphene structures. (e) and (f) Microstructures of the resulting interconnected 3-D graphene materials with very well defined pore structures [34]. Reprinted with permission from reference 34. Copyright 2015 John Wiley and Sons; (g) An illustration ofthe development of porous metal oxides such as layered double oxides (LDO) using a calcination/reduction process. These materials were used as templates for graphene growth, by Zhang et al. Following the growth, the templates were etched away, in orderto obtain free standing 3-D graphene structures [36]. Reprinted with permission from reference 36. Copyright 2015 John Wiley and Sons; (g) SEM image of an opal substrate - an emerging substrate that has demonstrated potential as a suitable template for porous 3-D carbon growth [38]. Reprinted with permission from reference 38. Copyright 2014 John Wiley and Sons.

behind a porous framework of GO with an interconnected pore structure mimicking the shape of the PS spheres. These electri- cally conductive porous networks served as an excellent host to anchor MnO_2 catalyst particles for supercapacitor applications. The synthesis of porous carbon-based 3-D structures has also been accomplished using opals (Fig. 5h) as templates [38]. The proce- dure consisted of a thermolysis step where the opal substrate was immersed in mixtures of sucrose, pyrazine, sulfuric acid, and dis- tilled water at 80 °C for 6.5 h, followed by drying and annealing at 1000 °C. Finally, the resulting opal substrate was etched away with hydrofluoric acid, leaving behind a 3D porous N-doped carbon network. It was possible to tune the optical properties of these materials with varying the nitrogen concentration [38].The decom- position temperature in air also increased when increasing the N- content. Additionally, incorporation of nitrogen into the carbon network resulted in an increased electrical conductivity [38].

Impregnation based approaches toform composite sponges

Graphene-based structures can add functionalities when adding other conducting materials, such as TiN and MoS_2. For example, catalysts with enhanced electrocatalytic activity for hydrogen evo- lution reaction (HER) [40-42]. In this respect, Chang et al. reported the fabrication of MoS_x/graphene/3D Ni foams by a two-step process [43]. First, a porous 3-D Ni foam was subjected to CH_4/H_2 (in the ratio 15:100) vapors in a CVD setup at 1050°C and 500mTorr for 1 h. Graphene layers were then deposited on the Ni foam dur- ing this process. Subsequently, the graphene-coated Ni foam was dipped in an ammonium thiomolybdate ($(NH_4)_2MoS_4$) solution (5 wt% in DMF) and heated to 100 °C for 10 min. MoS_x layers were then deposited on the graphene/Ni after subsequent annealing at 100-300 °C in inert atmospheres. Another approach whereby graphene foams served as a support for anchoring MoS_2 nanosheets was demonstrated by Chen et al. in 2014 [44]. This method consisted of a single-step hydrothermal process where an aqueous solution of GO (prepared using a modified Hummer's method) was mixed with ammonium molybdate and thioacetamide and heated at 200 °C for 24h [44]. Fig. 6a shows a photograph of the GO dispersion mixed with the precursors, and the hydrogel obtained after performing the hydrothermal synthesis. Upon cooling the resulting hydrogel, freeze drying was carried out in order to obtain MoS_2/graphene multi- functional composites. Microstructures of these composites are shown in Fig. 5b and c. Raman spectroscopy of the composites confirmed the presence of a MoS_2 phase along with graphene layers (Fig. 6d).

Synthesis of CNT-Based three dimensional structures

Since the structural identification of carbon nanotubes (CNTs), they have been widely studied due to their exceptional properties. There are many different techniques that have been developed to create 3-dimensional networks of CNTs, particularly over past five years. Below, we outline and categorize the most relevant tech- niques in the following sections.

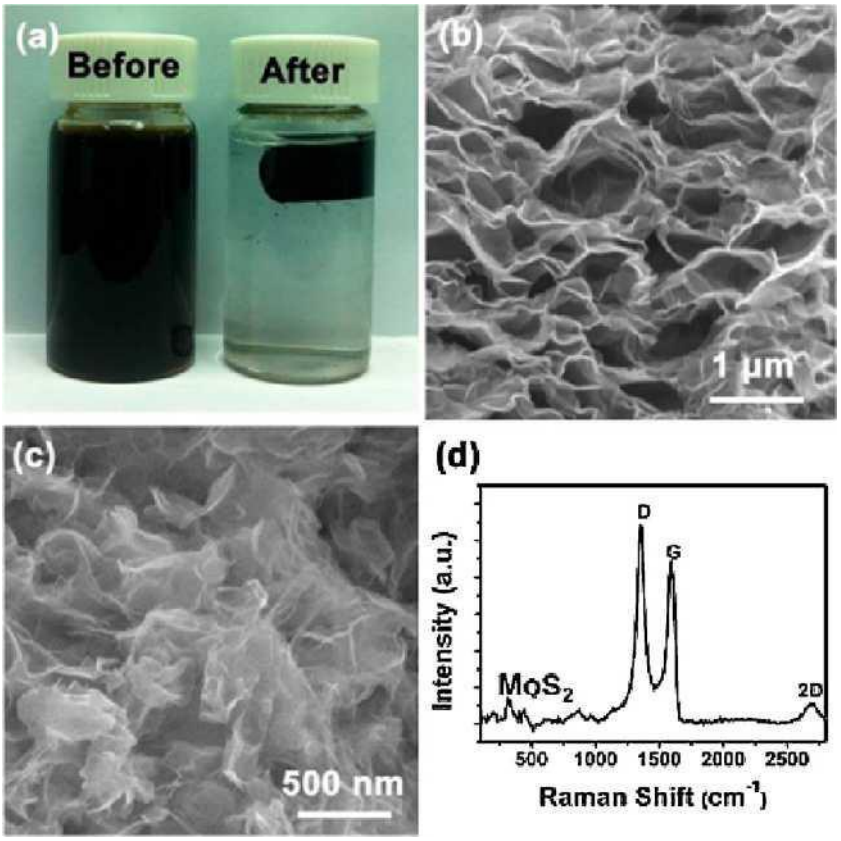

Fig. 6. (a) A photograph showing the precursor solution and the end-product during the preparation of composite hydrogels of graphene and M0S2 using a hydrothermal process. (b) and (c) Microstructure of the graphene/MoS2 composites as seen under a SEM. (d) The presence of MoS2 in the composite was confirmed by observing its characteristic peak(~313.5cm^{-1})inthe Raman spectrum acquired from the material [44]. Reprintedwith permission from reference 44. Copyright 2014AmericanChemical Society.

Growth ofCNT networks by Chemical vapor deposition: sWNTs, MWNTs, and the effect ofdopants during growth

CVD has proven to be a versatile and scalable technique not only for the growth of 1D CNTs and 2D graphene, but also 3-D structures composed of these building blocks. This has been achieved using porous 3-D templates, as well as by the addition of dopant atoms such as boron, sulfur and nitrogen during growth [45-48]. Freestanding 3-D sponges made of highly entangled MWNTs were synthesized by Gui et al. using CVD in 2010 [49]. The CNT sponges were grown inside a quartz tube by pyrolizing 1,2 dichlorobenzene and iron catalyst at 860 °C. The thickness ofthese CVD synthesized sponges were found to depend on the time of the CVD reaction. Other reports on CVD synthesis of macroporous sponge-like 3- D structures of CNTs are by Hashim et al. and Shan et al., who employed non-carbon species at low concentrations (<1 at.%) to modifythe tubularmorphologyofCNTs [45,48]. For example, boron atoms, when added during CNT growth, enable the formation of "elbow-like" kinks on the tubes, and cause entanglement and interconnections of these tubes, thus resulting in macro porosity (see Fig. 7a-d). By careful control of the doping levels, these authors demonstrated that CNT growth can indeed be tuned to obtain 3-D structures.

The CVD process offers some advantages over solution-based processing methods when growing 3-D porous CNT structures, such as being fast and scalable. Recently, Duong et al. reported a floating catalyst-based CVD route to grow CNT aerogels in a contin- uous manner [50]. The authors used methane as the carbon source, ferrocene as the catalyst, thiophene as the growth promoter, and hydrogen as the carrier gas, and performed CVD synthesis within a quartz tube reactor at 1200 °C. The CNTs were deposited on a substrate kept in the cold zone of the quartz tube, where the temperature was around 300 °C (Fig. 7e and f). Using this method, they were able to engineer the densities of the resulting CNT aerogels to obtain lightweight materials which could reach very low densi- ties, comparable to the lightest graphene aerogels reported so far (~0.55 mg cm^{-3}). However, it still remains a challenge to be able to precisely control a periodic pore structure using CVD without using templates.

A two-step CVD process is another technique employed to form covalent CNT junctions[51]. Recently, in our group we have produced large-area (cm^2-scale) networks of individually inter- welded CNTs by exposing previously synthesized nanotubes to a secondary CVD process in presence of Fe nanoparticles. In this method, several dry-state drawn sheets of preferentially aligned CNTs are overlapped onto each other and wrapped around perforated-pyrolytic graphitic substrates that are later exposed to the CVD of ethanol at 950°C in an Ar/H_2 (15%) atmosphere. Such a process results in the formation of a continuous CNT framework with clearly identifiable X-, Y and T-junction-like morphologies (Fig. 7g and h). While we are still studying the mechanical and structural properties of this material, we envisage it might have an important impact for future practical applications, such as heat transport applications [52] or composite reinforcement [53].

Sponges obtainedfrom CNT suspensions

Low density CNT-based 3-D structures have been synthesized using various approaches, particularly using their dispersions as raw materials. Most of the reports on self-assembly of CNTs use

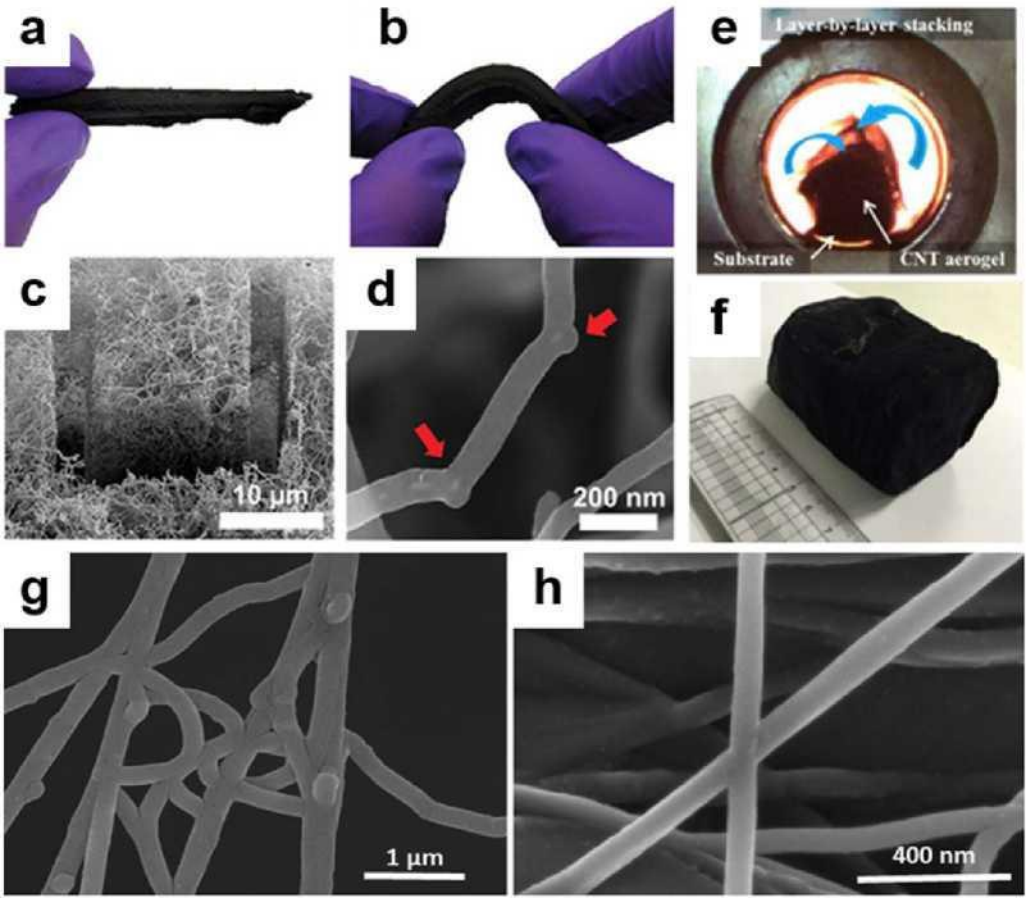

Fig. 7. (a) and (b) Macroscopic view of a flexible boron-doped CNT sponge synthesized using CVD. (c) and (d) SEM images showing their intricate microstructure, especially the high degree of entanglement observed among the tubes. The boron atoms help to modify the tubular structure in order to form "elbow-like" features indicated by the red arrows [45]. Reprinted with permission from reference 45. Copyright 2012, Nature Publishing Group; (e) A photograph of CNT sponge being formed within the hot zone and collected in the cold zone of a CVD furnace using the conditions reported by Duong et al. (f) A free-standing CNT sponge after collecting it from the cooled down reactor [50]. Reprinted with permission from reference 50. Copyright 2016, Elsevier Ltd.; (g) SEM image of multiple nanotubes junctions obtained via nanoscale welding; (h) High magnification SEM image ofan individual junction with "X' morphology. (For interpretation ofthe references to colour in this figure legend, the reader is referred to the web version of this article.)

gelation agents to establish cross-links among tubes [54]. A typi- cal process for creating CNT-based aerogels involves acid treated or functionalized CNTs with a chemical cross-linker, followed by a drying step. Additional annealing treatments on the dried aerogels have also been reported to improve their mechanical stability, and in some cases, their electrical conductivity [26]. Polymers such as poly(3-(trimethoxysilyl) propyl methacrylate) (PTMSPMA) and ferrocene-grafted poly(p-phenyleneethynylene) (Fc-PPE) have been used for CNT aerogel fabrication by some groups to form very light-weight aerogels (~4mg/mL) (Fig. 8) [26,55]. Apart from polymers, some of the other gelation agents that have demonstrated capacity to cross-link CNTs are amino acids and organogelators [56-58].

Although gelation of CNTs assisted by chemical cross-linkers is now being widely studied, other routes have also been established to fabricate CNT aerogels. For example, a very simple technique was demonstrated by Bryning and coworkers in 2007, in which SWNTs were solubilized in an aqueous solution with a 5:1 wt ratio of sodium dodecylbenzene sulfonate (NaDDBS) surfactant. After heating the solution to 90 °C in a water bath for 3-5days, the authors were able to obtain a gel, which upon flash freezing in liquid nitrogen followed by freeze-drying, was converted into lightweight aerogels [59]. Interestingly, aerogel forming techniques without involving chemical cross-linkers possess large surface areas [60].

However, the complete removal of surfactants, even after heating the aerogels, is still very challenging, and results in deteriorating the intrinsic properties of CNTs. Hence, a novel surfactant free approach for the self-assembly of CNTs to form 3-D monoliths was explored by Pint et al. using electrophoretic deposition [61]. In this approach, electro-deposition was carried out by dipping a porous Ni foam in a SWNT solution and connecting it to the negative terminal of a power source. A counter electrode was connected to the positive terminal, and on supplying a potential drop across both the electrodes, CNTs were deposited on the nickel foam. After the deposition, the Ni foam (coated with CNTs) was allowed to dry for 12h and then treated with HCl for 48 h to etch away the Ni, resulting into a self-standing monolith of porous CNTs.

Synthesis of 3-D graphene-CNT hybrid structures

Reinforcing 2D graphene with its 1D counterpart (CNTs) are finding increasing applications for adsorption and purification [62-64]. The key is to engineer a truly hybrid system and obtain enhanced electrical and thermal conductivities, mechanical robust-ness, as well as larger active surface areas. Some of the works in this regard have focused on obtaining hydrogels consisting of mixtures of GO and CNTs, followed by drying techniques [65]. However, Gao et al. recently fabricated ultra-light weight graphene-CNT hybrid aerogels eliminating the hydrogel formation step [66]. Their

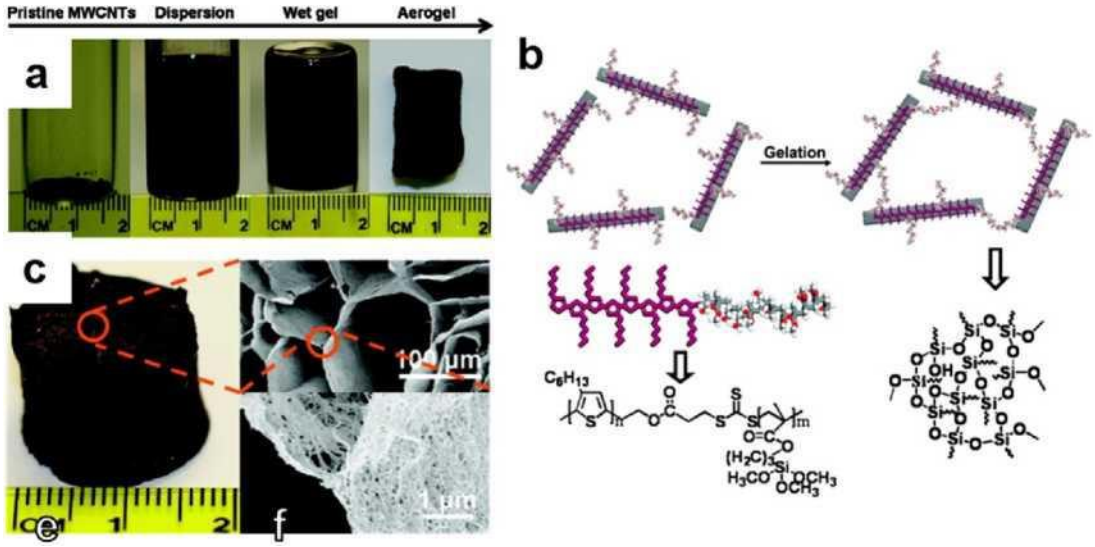

Fig. 8. (a) MWNT aerogel fabricated via gelation of a MWNT dispersion using PTSPMA polymer. (b) A schematic of the gelation process is shown. (c) A photograph of the aerogel and SEM images showing a honeycomb-type porous structure with MWNTs decorating the pore walls [55]. Reprinted with permission from reference 55. Copyright 2010 American Chemical Society.

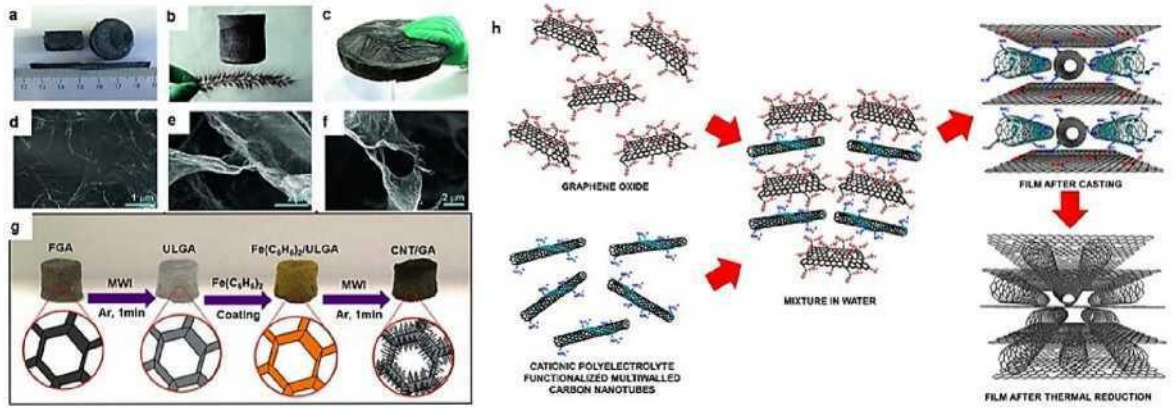

Fig. 9. (a)-(c) Photographs ofultra-flyweight graphene/CNT aerogels fabricated using cryo-dessication followed by a reduction of a GO—CNT aqueous solution mixture. (d-f) Microstructure of the composite material showing graphene layers interspersed with CNTs [66]. Reprinted with permission from reference 67. Copyright 2013 John Wiley and Sons; (g) A schematic illustration of using ultra-light graphene aerogels (ULGA) as substrates for CNT growth via catalyst deposition and microwave irradiation (MWI) [67]. Reprinted with permission from reference 67. Copyright 2014 American Chemical Society; (h) A novel fabrication process of CNT-graphene hybrid films making use of electrostatic interactions between cationic polyeltrolyte functionalized CNTs and GO in an aqueous solution. CNT-graphene hybrid structures are obtained after an annealing process [70]. Reprinted with permission from reference 70. Copyright 2013 American Chemical Society.

process involved cryo-dessication (or freeze-drying) of aqueous solutions of GO and CNT, followed by a reduction treatment with hydrazine vapors. These materials are highly porous, possess tun- able densities that depend upon the concentrations of the GO and CNT solutions, and are super oleophilic, being able to absorb oils up to 900 times their own weight (Fig. 9a-f). Another suit- able approach for fabricating CNT-graphene hybrids is by using graphene aerogels as templates for CNT growth. This was demon- strated by Qui et al., when coating graphene aerogels with ferrocene catalyst particles, and subjecting them to microwave irradiation (Fig. 9g) [67]. During the irradiation process, the heating of the fer- rocene particles causes their decomposition to iron particles and cyclopentadienyl, which served as the catalyst and carbon source for CNT growth respectively. The incorporation of CNTs into the graphene aerogels also increases their hydrophobicity (measured from differences in their contact angle with a droplet of water on their surfaces).

Other routes involve the reduction of hydrogels of GO and CNTs, particularly using metal cations such as Fe^{2+} [62,68].The metal ions not only help reducing the GO via charge transfer, but also prevent aggregation of GO layers by serving as spacers between the layers. They also help anchoring the CNTs between the graphene layers. While aerogels of CNTs and graphene are becoming increasingly popular for adsorption and as matrices for the fabrication of novel composites for energy applications, there is also some interest to utilize their assemblies as purification and filtration membranes [69]. One of the methods used to produce these membranes has been reported by Goh et al., using pressure assisted filtration of a GO - CNT solution mixture. This ensures intercalation of CNTs between the graphene layers and efficient anchoring of the tubes due to the TC-TC interactions between the materials.

Recent works have shown that it is possible to manipulate the electrostatic interactions between MWNTs and polyelectrolyte treated CNTs to obtain a layer-by-layer self-assembly in a 3-D stacked format [67]. Another interesting work carried out to obtain CNT-graphene hybrid 3-D foam is by Dong et al. who used a two step process [64]. In the first step, porous Ni foams were used as supports to grow graphene during CVD. Following this, the graphene

Table 1
Survey of synthesis methods and physical properties of currently reported 3-D graphene/CNT network solids.

Ref.#	Synthesis method	Surface characteristics	Contact angle	Mechanical properties	Electrical/electrochemical characteristics
[18]	Solvothermal reaction of GO sheets in alcohol	Void volume 99.9% or higher	135°	Near zero Poisson ratio for compression in both axial and radial direction	No change in electrical conductivity (0.4-0.8 Sm^{-1}) up to 90% compression
[21]	Reduction and self-assembly of GO with ethylene diamine	Estimated porosity 99.6%	155°	Supports static loads over 13,000 times its mass	Electrical resistance 2.48 Kilo-ohm without deformation, compression decreases resistance
[23]	In situ polymerization of acrylamide with GO	Specific Surface Area (SSA) 22.5-27.8 m^2 g^{-1} pore size 10-11.5 nm pore volume 0.07-0.09 cm^3 g^{-1}		Maximum compressive stress at 80% strain (the first compression) is 0.019-0.058MPa, depending on the density and polymer content of aerogel	Electrical conductivity 12-17 Sm^{-1}, depending on the density and polymer content of aerogel
[25]	Hydrothermal reduction of GO with Pyridine	SSA 236-361 m^2 g^{-1}, pore size 4.7-10.5 nm, total pore volume 0.28-0.95 cm^3 g^{-1}			Specific capacitance 162-179Fg^{-1},atthe current density of 0.5 Ag^{-1}
[27]	Hydrothermal reduction of emulsion of GO and hexane	SSA 310-490m^2g^{-1}		Compressive modulus 16.83-42.29 kPa, depending on the density ofthe aerogel	Electrical conductivity 0.48-1.76Sm^{-1}, depending on the density of the aerogel
[28]	Reduction ofGO by ascorbic acid, followed by directional-freezing and freeze-drying			Maximum compressive stress at 50% strain 14.1 kPa, forthe aerogel density of6.1 mg cm^{-3}	The electrical resistance of the aerogel is strongly dependent onthe deformation that it varies from 3400 to 82 ß as the strain varies from 0 to 83.7%
[34]	CVD with CH4 on sacrificial Ni template	pore size 20 ^m skeleton size 40 ^m			60-80 Scm^{-1}
[37]	Polymer foam template and ethanol flame	Pore volume 98.7%	142°	Elastic modulus 1.4-3 kPa, maximum compressive stress at 50% strain 0.3-2.3 kPa, depending on density	Conductivity up to 10 Sm^{-} achieved via annealing
[68]	One step reduction ofGO and formation of GO—CNT hydrogel in presence ofFe	SSA 315 m^2 g^{-1}	147.6°		
[69]	Reduction of GO by HI and subsequent assembly with CNTs	Mean pore diameter 0.96-1.29 nm	90° -60°		
[81]	Template directed hydrothermal carbonization process	SSA up to 547 m^2 g^{-1}	135.8°	Maximum compressive stress 85 kPa before fracture	
[82]	Hydrothermal reduction of GO in presence ofFe2O3	SSA 284m^2g^{-1}			High capacity of 1062 mA hg^{-1} at 100 mAg^{-1}, high rate capability and excellent cyclic stability over 100 cycles

coated Ni foams were immersed in a polyethylene glycol-ethanol solution containing 0.1 mM $Ni(NO_3)_2$ solution so as to decorate it with Ni particles that catalyze CNT growth in the second CVD step. When etching away the Ni foam, light-weight (<10mg/cm^3 bulk density), free standing monoliths of CNT-graphene hybrid foams were obtained. Hybrid structures of graphene and CNTs were synthesized using CVD by Gan et al. [71] These hybrid structures were created by growing graphene on copper foil pre-deposited with CNT films. The hybrid structure-n-Si device exhibited improved power conversion efficiency (PCE of 8.50%) over graphene-based (PCE of 6.46%) or CNTs-based devices (PCE of 5.93%) [71]. Another approach to create CNT-graphene oxide (GO) hybrids involved stacking of functionalized CNTs and GO in aqueous solution via electrostatic interaction (Fig. 9h) [70]. A sandwiched structure of rGO and CNTs, was successfully obtained after annealing. This hybrid structure exhibited lower conductivity and improved field-emission properties when compared to rGO or CNTs.

Properties of 3-D graphene/CNT network solids

A summary of synthetic approaches, as well as the electrical, mechanical and surface properties of 3-D graphene/CNT network solids are presented in Table 1. However, it is important to mention that structure, morphology and properties of these 3- D networks are often dependent not only on their 1-D or 2-D building blocks, but also on a variety of factors such as syn- thetic methods, precursors, functionalities etc. Even within the subcategory of graphene-based or CNT-based networks, different synthetic procedures, dimensions of the resulting networks and different measurement techniques, all give rise to a wide range

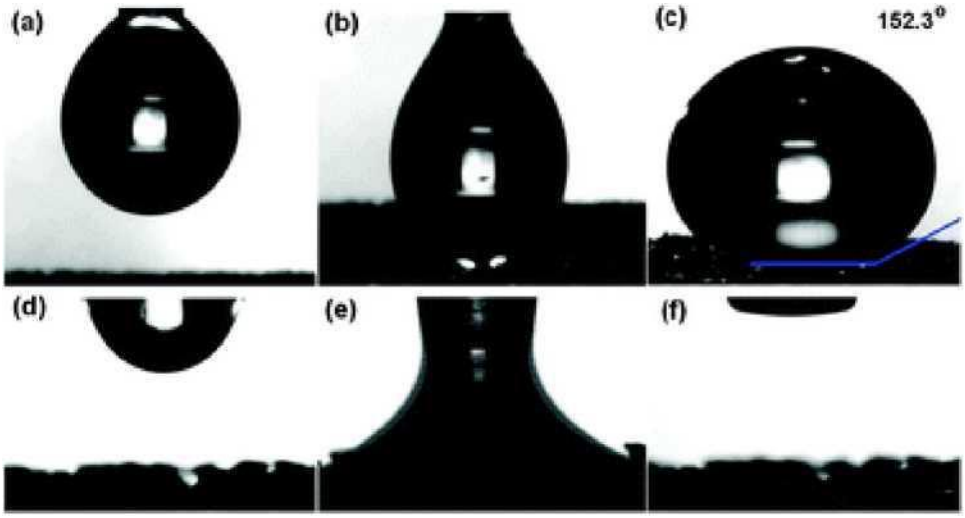

Fig. 10. (a)-(c) Video snapshots of wetting behavior of a water droplet, and (d)-(f) a compressor oil droplet placed onto the surface of graphene-CNT hybrid foam [64]. Reprinted with permission from reference 64. Copyright 2012 Royal Society of Chemistry.

of properties. From an environmental point of view, large sur- face area, continuous porous networks, hydrophobicity, structural flexibility, and mechanical robustness are attractive properties for adsorption applications. In this regard, Wu and coworkers reported lightweight and superhydrophobic pristine CNT sponges synthesized by CVD, with a contact angle of 156° for water droplets [72]. These sponges can be compressed to more than 95% volume reduction (e>95%) at low stress values (<0.25 MPa). In addition, Dong et al. [64] synthesized a 3-D graphene scaffold wrapped with CNT forests that demonstrated superior hydrophobicity (0 = 152.3°; Fig. 10a-c) as compared to 2D graphene (89.4°), 2-D CNT networks (98.2°), and 3-D bare graphene (108.5°). The improved hydrophobicity in 3-D analogues was attributed to the presence of air pockets located within the porous structure, as formulated by the Cassie-Baxter surface model [73]. The hydrophobicity was further increased in the hybrid foam due to the nano-roughness created by the CNT forest on the graphene surface and the air interfaces in the nanoscopic voids within the CNT forest. On the contrary, an oil droplet spreads quickly and was then completely absorbed by the hybrid foam (Fig. 10d-f). Thus, apart from being superhydrophobic, the graphene-CNT foams exhibited superoleophilicity (perfect oil wetting, as evidenced by (0 = 0°).

Their excellent electrical properties make them useful for electronic device applications, such as batteries, solar cells and electrochemical sensors. If ohmic junctions can be formed between these individual components, the superior electrical properties should be carried over into all three dimensions. It is notewor- thy that remarkable bulk electrical conductivities (~1 x 10^2 S/m) were obtained in 3-D aerogels formed by the sol-gel polymeriza- tion ofresorcinol and formaldehyde containing suspended GO [74]. These conductivities were two orders of magnitude higher than graphene assemblies with only physical cross-links such as van der Waals forces (~5 x 10^{-1} S/m) [17]. Further improvement in elec- trical conductivity was obtained by employing alkali treated GO [75]. The excellent electrical conductivity of these 3D structures are often coupled with surface functionalization by nanoparticles for catalytic applications. For example, high catalytic efficiency for the electrochemical oxidation of methanol was achieved by sur- face functionalization of conducting graphene foams containing Pt nanoparticles [76]. As mentioned in previous reports, CNT sponges typically exhibit higher electrical conductivity than graphene- based sponges when both are obtained from aqueous suspensions. However, the use of CVD techniques may provide graphene-based 3-D structures with higher electrical conductivity, even exceeding that of CNTs [8].

3-D structures of CNT and/or graphene possess excellent mechanical stability, strength and flexibility which are attractive features for many environmental applications. For example, CNT sponges synthesized using the CVD technique reported by Gui et al. show tunable compressibility over a wide range depending on the material density and compressive stress [49]. The lower- density sponges (5.8 mg cm^{-3}) exhibit high compressibility of up to 90% volume reduction under a stress of 0.1 MPa, while the higher-density sponges (25.5 mg cm^{-3}) can recover to 93% of original volume after compression. CNT sponges with a truss-like struc- ture, recently reported by Dai et al., exhibit a combination of super elasticity, high strength to weight ratio, fatigue resistance, thermo-mechanical and electromechanical stability, due to cova- lent interconnections established among CNTs [77]. Compressive stresses were recorded as a function of increasing strain (10% up to 90%) for these sponges; and the slopes of the linear portion of the curves remained almost constant for different strain values, thus indicating a negligible degradation of mechanical strength. These materials exhibited identical stress-strain behavior after 1000 cycles at 400 °C, and similar cyclic behavior was observed at -100°C and 35 °C (Fig. 11a). This outweighed the thermomechan- ical performance of conventional polyurethane sponges. Coating inelastic aerogels of SWNTs with one to five layers of graphene nanoplates can transform it into a superelastic material, as demon- strated by Kim et al. [78]. The graphene-coated CNT aerogels exhibit elastic recovery when compressed up to 60% strain and higher, whereas the CNT aerogels undergo plastic deformation beyond 10% strain. Wu et al. synthesized solvothermally graphene sponges that revealed excellent thermal and mechanical stability over a wide temperature range (-196°C to 900 °C), thus indicating the presence of strong cross-linking among the GO layers within the sponges [18]. A combination of properties such as densities similar to air, near-zero Poisson's ratio in all directions, and the ability to reversibly recover elastically from large-strain cyclic compressions (up to 98% compression in air and 90% in liquids) (Fig. 11b and c), make these novel sponges unique. However, the strength of these sponges under tension does not match their performance in com- pression. When uniaxially pulled beyond 5% strain, they tear apart via crack propagations.

Regarding theoretical studies of mechanical properties, Miller et al. [79] examined four different families of triply periodic min-

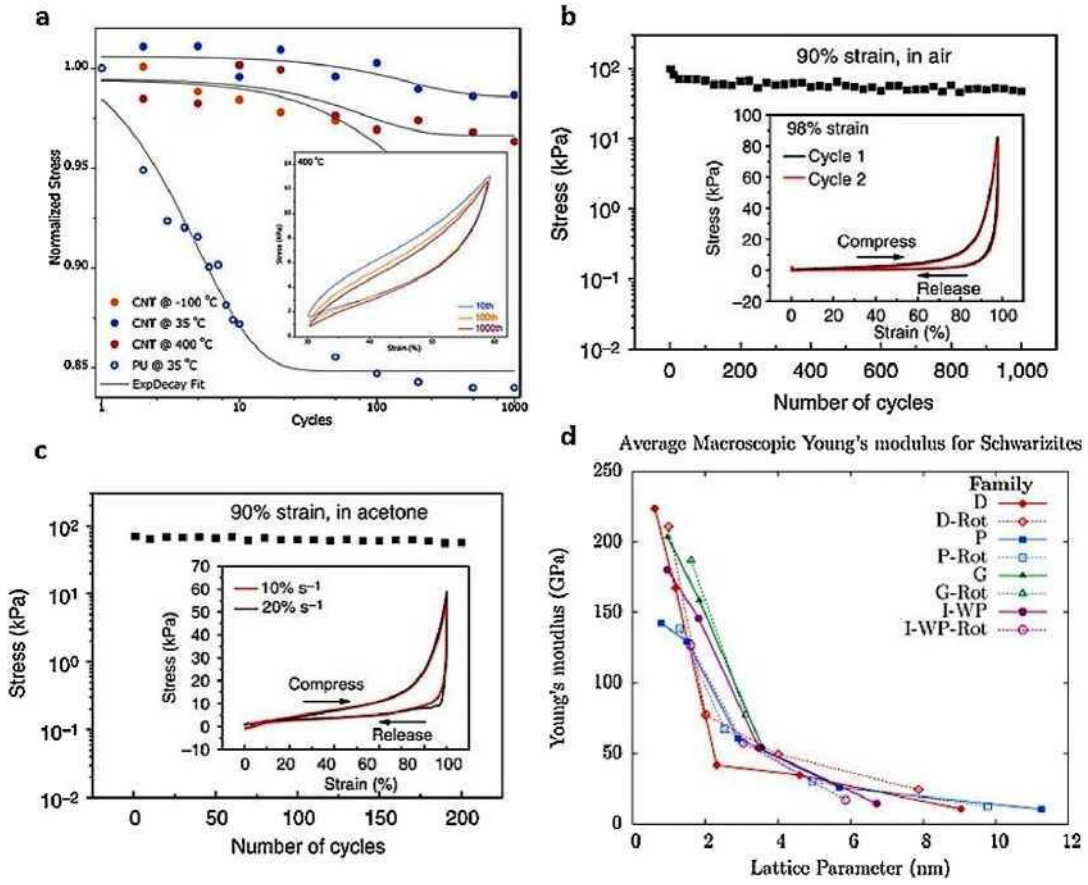

Fig. 11. (a) Measured compressive stress response at a strain of 60% with respect to number of cycles, Inset: compressive cyclic testing of CNT sponges at 30-60% strain, 0.016 Hz, 400° C, for the 10th, 100th and 1000th cycles [77]. Reprinted with permission from reference 77. Copyright 2016 Nature Publishing Group; (b) The compressive stress to reach 90% strain at an engineering strain rate of 40% strain s^{-1} is plotted as a function of cycle number for 1000 cycles in air. The inset shows the reversibility of stress-strain curves fortwo successive cycles in air(black and red curves, respectively) up to a compressive strain of98% [18]. Reprinted with permission from reference 18. Copyright 2015 Nature Publishing Group; (c) The compressive stress needed to reach 90% strain at an engineering strain rate of 20% strain s^{-1} is plotted as a function of cycle number for 200 cycles. The inset shows stress-strain cycles in acetone up to 90% strain for engineering strain rates of 10% strain s^{-1} (red line) and 20% strain s^{-1} (black line). (d) Decrease ofcalculated Young's moduli with increase of lattice size [79]. Reprinted with permission from reference 79. Copyright 2015 Elsevier Ltd. (For interpretation of the references to colour in this figure legend, the reader is referred to the web version of this article.)

imal surfaces (TPMS) decorated with graphene, with very high ratios of hexagons to rings with more than six atoms. TPMS sur- faces display saddle shapes at every point and are also periodic in three dimensions. The four families exhibiting such non-positive Gaussian curvatures studied in this paper were the Primitive (P), Diamond (D), Gyroid (G), and I-graph - Wrapped Package graph (I-WP, where I-graph is the symmetric graph of degree eight, con- structed by joining by an edge all nearest neighbor points of a bcc lattice; WP-graph is constructed by joining by an edge the centers of opposite edges of each square face of every cube in a space fill- ing assembly of cubes [80]) surfaces; all resembling 3-D graphene foams. Fig. 1g show the molecular structures belonging to the P8- 1 and I-WP8-1 (8 refers to the introduction of octagonal rings, followed by 1, which is the minimal number of hexagonal rings sep- arating two octagonal rings) varieties calculated using the Surface Evolver code. The energetics, elastic stability and mechanical properties such as Young modulus, bulk modulus and Poisson ratio were obtained using density functional theory (DFT) and empirical meth- ods. The bulk and Young moduli decrease as these structures grow in size (Fig. 11 d).The calculated values of average macroscopic Pois- son's ratio for the D-, P-, G- and I-WP Schwarzite families are still not as low as those observed in the graphene foams experimentally obtained from GO by Wu et al. [18], possibly because of the presence of defects in GO (e.g. topological, vacancies, edges, etc.). The P and I-WP geometries favor smaller average values of Poisson's ratio for the entire cubic cell and are more likely to be synthesized experimentally. The authors further demonstrated that for the giant D Schwarzite with ripples, the Poisson's ratio decreases and becomes negative. Negative Poisson ratio materials with graphitic structures constitute a fascinating new possibility that requires further experimental and theoretical investigations.

3-D graphene/CNT network solids for pollution management

3-D graphene/CNT networks show fascinating prospects in the removal of pollutants from contaminated water and air for the following reasons. First, the 3-D structures based on CNT and graphene consist of high surface area networks with micro-, *meso*- and macro-pores that facilitate diffusion and transport of pollu- tant molecules and ions. Second, their integrated morphology not only offers effective pollutant separation and recycling, but also minimizes potential environmental risks caused by the acciden- tal release of CNTs and graphene sheets [83]. Third, these 3-D solids are highly stable and can be employed in various aque- ous environments including harsh acidic conditions [84] and wide temperature ranges [81]. Consequently 3-D graphene/CNT networks have been thoroughly investigated for water filtration, water/oil separation, oil-spill clean-up, wastewatertreatments and detection/adsorption of toxic air pollutants. Apart from adsorp-

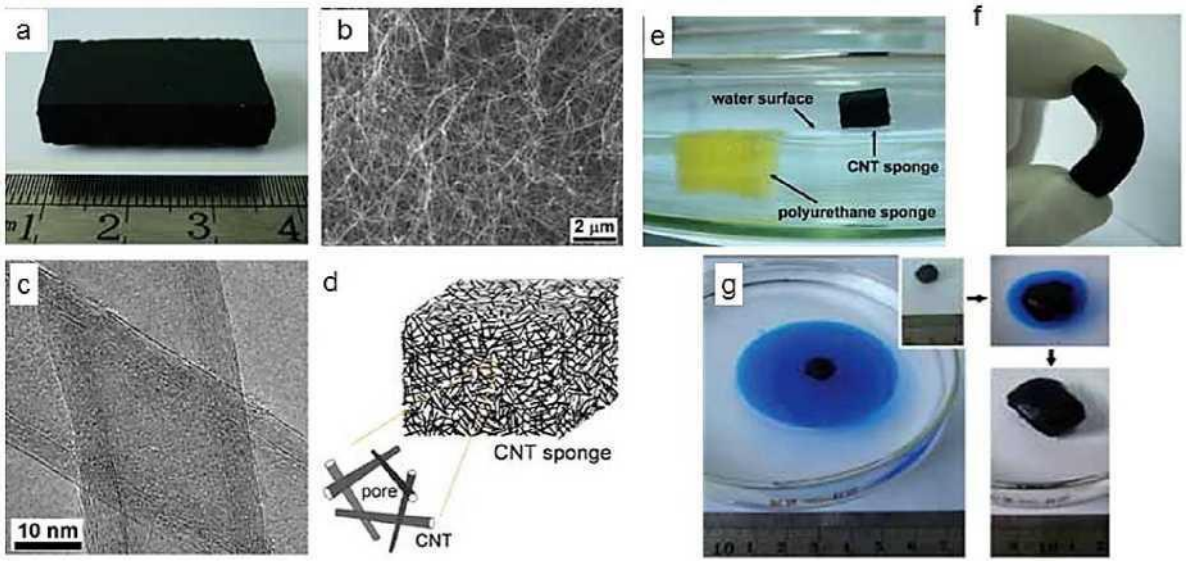

Fig. 12. (a) A monolithic sponge with a size of 4 cm x 3 cm x 0.8 cm. (b) Cross sectional SEM image of sponge showing overlapping CNTs. (c) TEM image oflarge cavity, thin walled CNTs. (d) Illustration of the porous structure of the sponge. (e) Picture of floating CNT sponge and sinking polyurethane sponge in a water bath. (f) A CNT sponge bent to arch shape showing mechanical robustness. (g) Adsorption of vegetable oil film (dyed in Oil Blue) by CNT sponge [49]. Reprinted with permission from reference 49. Copyright 2009 John Wiley and Sons. (For interpretation ofthe references to colour in this figure legend, the reader is referred to the web version ofthis article.)

tion related applications, 3-D graphene/CNT networks also serve as platforms for the fabrication of exotic catalysts in pollution, for example, in the photodegredation of water pollutants. In the following sections different environmental applications of 3-D Graphene/CNT networks will be discussed in detail.

Adsorption ofoil and organic solvents

Over the past few decades accidental release of oils and organic solvents during extraction, transportation and storage have resulted in an adverse impact on marine and land ecology. In order to address this issue various sorbent materials have been developed such as crosslinked polymers and resins [85,86], fibers [87], polymer gels [88,89], nanocomposites [90], organic-inorganic hybrids [91], silica [92] and carbonbasedmaterials [8,93].However, these materials possess certain drawbacks. For microporous polymers with large specific surface area, even though high adsorption capacity is achievable, the production cost is high and their environmental risks are still unclear [94]. For carbon based sorbents, exfoliated graphite with low bulk density has demonstrated rapid oil adsorption (i.e. within 2 min) up to 86 times its weight [95], but, it does not exhibit high adsorption capacities for organic sol- vents and its powdered texture leads to difficult separation process and low recyclability. In this context, Gui et al. [72] fabricated CNT sponges that can be used more than 1000 times without significant changes in structure, hydrophobicity and adsorption capacity. The sponges consisted of self-assembled interconnected CNT networks (Fig. 12a-d) with an estimated porosity >99%, pore sizes ranging from several nanometers to few micrometers, and a density ranging between 5 and 10 mg cm^{-3}. The sponges exhibit contact angles of about 156° for water droplets, and could float on water owing to their low density. In comparison, a conventional polyurethane sponge was hydrophilic and sank below the surface level of water (Fig. 12e). Moreover, the CNT sponges had excellent structural flex- ibility (Fig. 12f) and remarkable mechanical properties such as large strain deformation with almost full volume recovery and resistance to structural fatigue under cyclic stress conditions in oils. Adsorption of vegetable oil by a spherical monolith of this sponge, when placed in an oil-water mixture is shown in Fig. 12g. The adsorption capacity of the CNT sponges ranged from 80 to 180 times their own weight for various oils and solvents, several times higher than polymeric sponges and activated carbons. The high adsorption capacity and fast adsorption rate resulted from physisorption of organic molecules that could be stored inside sponge pores. The adsorbed oils and solvents could be salvaged by mechanical compression. Those could also be directly burned in air without significantly affecting the sponge properties, mainly due to the high porosity of the macrostructure allowing a quick diffusion of the generated heat.

Similar to CNT sponges, graphene-based macrostructures have shown great potential in the field of oil and organic solvent adsorption due to their ultra-lightness, high compressibility, high specific surface area, abundant porosity, hydrophobic TC-TC stacking interactions and ability of surface functionalization. The aromatic solvents generally show higher affinity for graphene-based sorbents than aliphatic solvents due to strong TC-TC stacking interactions [96]. In a seminal work published by Zhao et al. [97], an ultralight (density 2.1 ±0.3mgcm^{-3}) Nitrogen-doped 3-D graphene framework (GF) (Fig. 13a and b) was synthesized by hydrothermal treatment of graphene oxide and pyrrole. The ultralow density was ascribed to the rich open pore structures interpenetrating the graphene skeleton (Fig. 13c and d). GF could adsorb oils and organic solvents up to 200-600 times its own weight, which was much higher than ear- lier carbon-based sorbents such as graphene foams (10-37 times), graphene sponges (20-86 times), aerogels (13-27 times), carbon nanofiber aerogels (40-115 times) and CNT sponges (80-180 times). GF also exhibited a high adsorption rate of 41.7gg^{-1} s^{-1}, higher than previously reported for pure graphene and graphene aerogels (Fig. 13e and f).

Despite hydrophobicity of graphene nanosheets, the high cavity content and appropriate pore size in graphene-based macrostructures can cause some water adsorption [98]. In this context, synthesis of hybrid networks of graphene and CNTs can be useful. CNTs can be employed to increase the robustness and surface roughness of graphene sheets which attribute to better hydrophobicity and adsorption capacities. In 2014 Kabiri et al. [68] demonstrated a green and single step approach for the synthesis of 3-D graphene/CNT networks. The reduction of GO to graphene and the formation of a graphene/CNT network hydrogel were achieved in the presence of ferrous ions and heat. The prepared aerogels

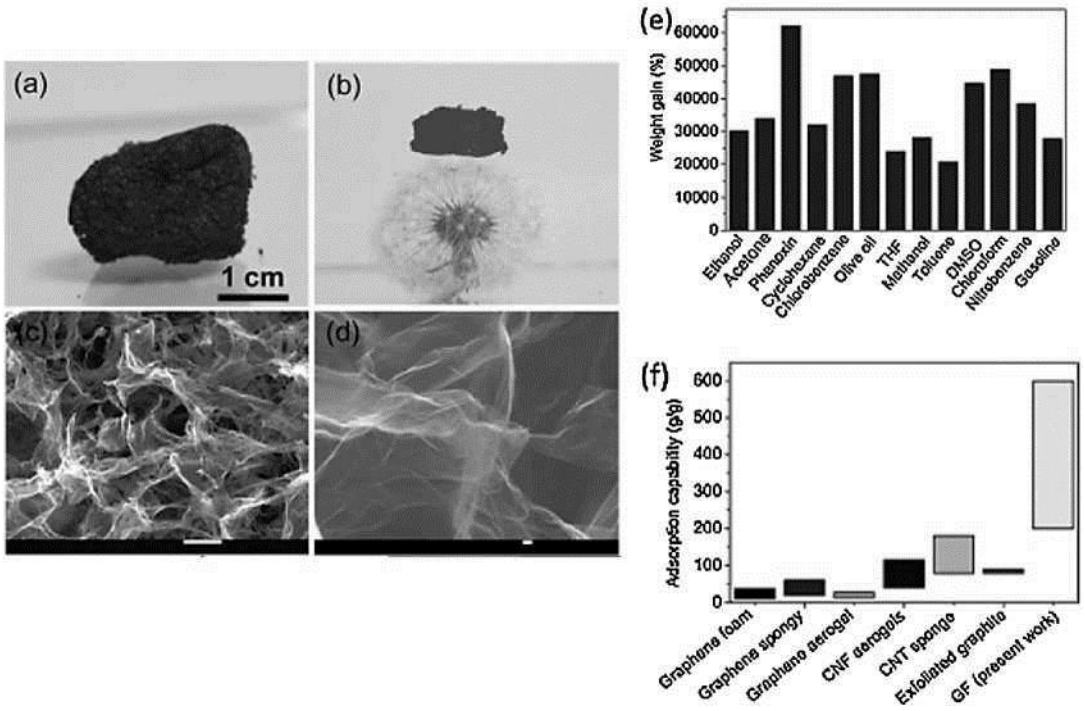

Fig. 13. (a,b) Photographs ofanas-prepared superlight GF and onewitha piece ofGFsize of 1.8 cm x 1.1 cm x 1.2 cm standing onadandelion. (c, d)SEM images ofthe sample in (a) showing graphene sheets and porous structure (scale bar 10 |xm and 100 nm, respectively). (e) Adsorption capacity of GF in terms ofweight gain. (f) The comparison of adsorption capacities of different carbon based materials [97]. Reprinted with permission from reference 97. Copyright 2012John Wiley and Sons.

exhibited outstanding adsorption performance for the removal of petroleum products, fats and organic solvents especially under continuous vacuum regime showing adsorption capacity of 28 L of oil per gram of aerogel in a non-turbulent water-oil system [68].

Another increasingly popular variation in designing CNT/graphene-based sorbents is to decorate these sponges with magnetic nanoparticles [45,49]. Magnetic sorbents have advantages since they can be easily collected after saturation adsorption under magnetic fields. In cases of an accidental damage of the sorbent, all broken parts of the magnetic sorbent can be recovered in a safe and controllable manner. Thus, it can be concluded that 3-D graphene/CNT network solids are competitive candidates in the field of oil and organic adsorption, and their use should be scalable to industrial level. However, it is clear that further research is necessary in this area, for example, it is necessary to control the functional groups on the graphene surface in order to harness ultimate hydrophobicity and selective adsorption properties.

Adsorption of organic dyes

Disposal and management of organic dyes from dye manufacturing and textile industries is of great environmental concern. Many of these dyes and their breakdown products such as ben- zidine, naphthalene, etc. are toxic, carcinogenic or mutagenic to life forms. Most dyes are dissolved in either cationic (e.g. methy- lene blue (MB), methyl violet (MV), Rhodamine B (RhB), malachite green (MG) etc.) or anionic (e.g. methyl orange (MO), Bordeaux red (BR), rose Bengal sodium salt (RB), acid orange 7 (AO7) etc.) forms. Fortunately, the extensive surface area and abundant pore struc- tures of 3-D graphene/CNT solids allow diffusion and storage of dye molecules. Moreover, both electrostatic and TC-TC interaction can be exploited to take full advantage of such materials in regard of dye adsorption. As GO sponges can have negative surface charges owing to deprotonation of oxygen containing functionalities, they are expected to reveal extraordinary adsorption capacity for cationic dyes. Cheng et al. [99] demonstrated that poly-dopamine assem- bled graphene aerogels had better adsorption capacities for cationic dyes and benzene structure enriched moieties such as MB, MV etc. Xu et al. [15] synthesized hydrogel from self-assembly of GO and DNA which had high loading capacity (960 mg g^{-1}) for the cationic dye safranin O. The negative surface charges in both GO and DNA generated strong electrostatic attraction with positively charged safranin O, which revealed high adsorption capacity. Due to sim- ilar reasons, GO-biopolymer gels reported by Cheng et al. [100] demonstrated higher adsorption capacity for cation dyes MB and MV, when compared to anionic or non-ionic reagents. It is worth mentioning that the solution pH plays an important role in deprotonation of surface functionalities of graphene oxide sponges, and thus high pH values are preferred to enhance electrostatic interaction between adsorbent surface and cationic dyes. However, for anionic dyes, the graphene/CNT surface needs to be further modified in order to increase adsorption capacities. In 2013 Sui et al. [101] synthesized an amine rich hybrid structure consisting of GO sheets and poly (ethylenimine) (PEI), which showed excellent adsorption capacity (800 mg g^{-1}) for an anionic dye called amaranth, a value that is superior to that of other carbon materials. It was thought that the strong affinity of protonated amine groups toward the sulfonated groups of the dye provided the driving force for the adsorption.

With the advancement in adsorption research of 3-D graphene/CNT structures, constant efforts are now being made in developing all carbon nano-architectured membranes with improved water permeability and enhanced membrane selectiv- ity. In 2015 Goh et al. [69] created highly stable membranes by intercalating surface-functionalized small-diameter multi-walled carbon nanotubes (MWNTs) into rGO sheets that resulted in almost 100% rejection for three organic dyes of different charges (cationic MB, RhB and anionic AO7). Exceptional stability of these all carbon nano-architechtured membranes was demonstrated

when subjected to a turbulent cross-flow hydrodynamic condition of 2000 mL min^{-1} and a Reynolds number of 4667. From the mechanistic viewpoint, the exceptional stability resulted from van der Waals attraction forces and TC-TC stacking interactions between the assimilated rGO sheets and the nanoscale rGO foliates on the intercalated CNT anchors. In addition, the water permeability reached 52.7 Lm^{-2} h^{-1} bar^{-1},which is 4.8 times that ofthe pristine rGO membrane and five to ten times higher than most commercial nanofiltration membranes. However, studies concerning practical separation applications of 3-D graphene-CNT networks are still scarce and based on the advances made in this work, further research regarding smart porous membranes involving such networks is expected to occur in the near future.

Adsorption ofinorganic pollutants

Worldwide environmental concern is caused by heavy metal cations e.g. Cu^{2+}, Pb^{2+}, Cd^{2+} etc.; nonmetal anions e.g. fluoride, nitrate, sulfide, phosphate and anionic forms of heavy metals such as chromate, arsenite, arsenate etc. These elements and compounds can exhibit extreme toxicity, they can be non-biodegradable and have a tendency to be accumulated in the human body [102,103]. As mentioned above, 3-D graphene/CNT networks show fascinat- ing adsorption properties towards these pollutants. This adsorption process has been explained to be driven by three predominant mechanisms: *electrostatic interactions* [104,105], *ion exchange process* [106] and *surface complexation* [107,108]. For electrostatic interactions, oxygen functionalities on the adsorbent surface, that are negatively charged, attract heavy metal cations. In case of an ion exchange, H_3O^+ groups present in the adsorption sites are replaced by metal cations. For both of these mechanisms, similar to the case of cationic dyes, an increase of pH can improve adsorption capacity. However, it is also important to prevent the solution from reach- ing a high enough pH to precipitate metal hydroxides [104]. In this regard, Gao et al. employed 0.1 M HCl for the desorption of heavy metals from graphene hydrogels [107]. Apart from the pH value, temperature is also an important factor for the adsorption of metal cations. Since the adsorption of metal cations on a graphene surface is endothermic, higher temperature can be employed to achieve an enhanced adsorption capacity. In this context, the presence of het- eroatoms with lone pairs of electrons such as N, S, O can improve the adsorption capacity of metal cations on 3-D graphene/CNT structures via electrostatic interaction. Polymer-GO hybrid sponges are of increasing interest, and in this regard Zhang et al. [109] synthesized chitosan-gelatin/GO hybrid monoliths that were used for removal of Cu^{2+} and Pb^{2+}. It is noteworthy that the amount of additive needs to be carefully controlled so that no serious folding of GO sheets can take place, which could result in a decrease of the surface area and block the activity of the adsorption sites.

It is also worth mentioning that iron and iron oxide based nanostructures have shown high efficiency in the removal of heavy metals including As (III), As (V) and Cr (VI) [110,111]. However, their small particle size, instability and susceptibility to oxidation have limited their usage. By combining iron minerals and graphene/CNT networks, the aggregation of both carbon nanostructures and iron based nanoparticles can be prevented [82]. Moreover, heavy met- als can be trapped into the porous structures, and afterwards a facile separation would be achieved due to the intrinsic magnetic properties of iron nanoparticles.

Recently hybrid structures of inorganic layered materials and 3-D graphene are emerging as novel multifunctional adsorbents. In 2016, Liu et al. [112] fabricated 3-D graphene/8-MnO_2 aerogels via self-assembly and reduction of GO, followed by in-situ solution-phase deposition of ultrathin §-MnO_2 nanosheets. The resulting 3-D aerogels exhibited a fast adsorption kinetic rate as well as superior adsorption capacity toward heavy metal ions. The saturated adsorption capacities of graphene/8-MnO_2 aerogels were as large as 643.62mgg^{-1} for Pb^{2+}, 250.31 mgg^{-1} for Cd^{2+} and 228.46 mgg^{-1} for Cu^{2+}, calculated by the Langmuir isotherm model, which usually describes adsorption of heavy metal ions. It was noted by the authors that the heavy metal ions could not only adsorb on the surface of graphene/8-MnO_2, but also could intercalate between the interlayers of 8-MnO_2. This demon- strated the synergistic effect of the electrostatic attraction, surface complexation and ion exchange between heavy metal ions and pre-intercalated K^+ present in 8-MnO_2, supported by the expansion of its basic crystal structure after adsorption. The kinetics of the adsorption were fitted using a pseudo-second-order model, which is common in this context, indicating chemical adsorption involving covalent forces. It was further demonstrated that the regenerated aerogels after an initial HCl and subsequent KOH treatment, maintained their original shape and could be repeatedly used for more than eight cycles without obvious performance degradation, thus leading to the recyclability of the absorbents.

Gas adsorption and sensing

Gas adsorption by 3-D CNT/Graphene networks is a relatively unexplored area of research and only a small number of papers in last 2-3 years reported graphene foams as adsorbents of compounds such as acetone [113], CO_2 [101,114] and formaldehyde [115] . In a pioneering work by Sudeep et al. [114] chemically crosslinked GO foams demonstrated superior adsorption capacity for CO_2 (2.7mmol/g at 20atm pressure) when compared to many other carbon-based materials. Once again, high surface area and fast/versatile transport paths through interconnected pores in such foams attributed to the superior properties. However, the authors concluded that several of the macropores did not really contribute to the adsorption capacities and the micropores and mesopores present in the structures were the active sites for CO_2 adsorption. The adsorption took place mainly through weak van der Waals type interactions, which was supported by the good reversibility observed in the desorption measurements. This also facilitated an easy regeneration of the absorbent, making those foams superior to zeolites, another well-known CO_2 adsorbent with very high regeneration temperature. The authors also put forward that there could be a slight contribution to the CO_2 adsorption from chemical interaction between carbonyl groups present in the foams and CO_2 molecules. There are other reports demon- strating that surface functional groups can play an even more important role in gas adsorption. For example, CO_2 adsorption capacity of 3-D GO/PEI structures (11 wt%) was higher than GO foams without PEI (8 wt%), due to the interaction between CO_2 and primary/secondary amino groups present in GO/PEI macrostruc- tures [101]. Recently our group studied the adsorption capacities of boron doped (CB$_x$MWNT) and pristine 3-D MWNT sponge-like materials for CO_2, methane etc. Further analysis indicate that the surface areas, pore structures and active surface sites contribute synergistically towards enhancing their adsorption capacities.

High surface area graphene sponges have demonstrated their potential not only as gas adsorbents but also as gas sensors. Conducting graphene-based sponges can exhibit resistive and/or impedance changes upon gas adsorption, thus leading to a highly sensitive detection. Among one of the initial reports, Yavari et al. [116] demonstrated the use of robust CVD-graphene sponges to detect NO_2 and NH_3 gases. The sensor was able to reliably detect resistance change upon exposure to 20 ppm NH_3 and 20 ppm NO_2 gases at room temperature, with steady-state response times around 5-10 min. Desorption of the gas was achieved with joule heating. The sensitivity was an order of magnitude higher than that of conducting polymers [117,118]. The graphene sponge sensors also provide a less expensive gas detection method than semicon-

ducting metal oxide sensors that operate at higher temperature. Later, Alizadeh and Ahmadian [119] synthesizedgraphene aerogels using a hydrothermal reaction with various amounts of thiourea that exhibited a linear response in the resistance change for ammo- nia concentrations between 0.02-85 ppm. The limit of detection for these sensors was 10 ppb. The sensors were tested repeat- edly over an 8-month span and no significant change in response was observed, indicating good stability. The sensors were also tested in high humidity environments and demonstrated different results only in greater than 75% relative humidity environment. Feng et al. [120] recently studied the humidity sensing capabili- ties of graphene oxide foams with different thickness and oxygen content by measuring changes in impedance. Ultra-thin foams of less than 100 nm showed linear relationships between humidity and impedance change, while foams of greater thickness showed non-linear relationships. High sensitivity and high reproducibility were achieved between 11% and 95% humidity environments. Qi et al. [33] fabricated carbon nanotube-cellulose composite aerogels to study their sensing abilities for "volatile organic compounds" (VOCs) like methanol, ethanol, chloroform, and toluene. A dras- tic resistance change of up to 40% was documented for methanol, ethanol, acetone, chloroform, and tetrahydrofuran (THF).The polar nature of cellulose causes the dramatic resistance response when in contact with the mentioned polar compounds. It is worth not- ing that the authors were also able to demonstrate relative smaller resistance changes in response to other compounds like water, toluene, and hexanes (10-20%). Moving forward, gas adsorption and detection studies on 3-D graphene/CNT networks are yet to be extended to many other toxic gases such as CO, H_2S, SO_x, NO_x etc. From DFT calculations, nitrogen- and boron-doped carbon nanos- tructures show improved interaction for CO, NO, NO_2 and NH_3 gas molecules [121] and more experimental work needs to be per- formed in this direction with the interaction of these gases and their 3-D materials structures.

Catalytic conversion ofpollutants

High adsorption capacity is a prerequisite for the pollution transformation process. In addition, the electrically conducting 3-D networks of graphene/CNT ensure fast charge transportation and act as a suitable framework for dispersing the catalyst. When trans-forminggaseous pollutants, Long et al. [122] synthesized GO foams that had high adsorption capacity for SO_2 gas and catalyzed the oxidation of SO_2 to SO_3. Subsequently, the trapped SO_3 could be converted into H_2SO_4 upon exposure to water and hence could be separated via washing and filtration. In the process, GO foams par-tially reduced to rGO foams and their color changed from brown to black. In a later study in 2013, Huang et al. [123] demonstrated that La^{3+} and PEI crosslinked GO aerogels could oxidize high con-centrations of poisonous gases such as H_2S, SO_2 and HI into solids such as S, SO_3 and I_2, respectively, under ambient temperature and pressure. Thus, these sponges can potentially serve as alternative catalysts for conversion of gaseous pollutants as opposed to expensive noble metals or commercial carbons.

3-D graphene/CNT networks could also serve as an excellent platform for the degradation of aqueous pollutants with metal or metal oxide nanoparticles (NPs). A photocatalyst absorbs UV and/or visible radiation and the electrons in their valance band are promoted to the conduction band leaving behind holes. The electron-hole pairs generated in the photo-excited state migrate towards the surface where they can initiate redox reactions with the adsorbate. One of the limiting factors in the semiconductor catalysis efficiency is the rapid recombination of photogenerated electron-hole pairs. There are several reasons for utilizing 3-D graphene/CNT as a platform for such catalytic reactions: (a) as we have discussed earlier, an ample amount of aqueous contaminant is adsorbed into the 3-D network, (b) catalyst nanoparticles disperse uniformly onto the graphene/CNT surface which aggregate otherwise due to their high surface energy, and (c) the well- interconnected 3-D graphene/CNT structures provide enhanced charge transport preventing recombination of electron hole pairs and facilitate reactions with the contaminants. As a consequence, photodegradation activities of metal NPs such as Ni [124], Au [125] etc. and metal oxide NPs such as TiO_2 [126], SnO_2 [127], and CuO_2 [128] on 3-D graphene/CNT surfaces have been extensively studied. Graphene-TiO_2 composite, as a "rising star" material, is the most common photocatalyst used for the degradation of dyes and other pollutants. Zhang et al. [126] prepared TiO_2-grpahene nanocomposite hydrogels (TGH) that possessed higher MB adsorption capacity when compared to graphene hydrogels (GH) and TiO_2 nanoparticles. Moreover, under UV irradiation, degradation of MB could be completed in 30 min in the presence of TGH, whereas for TiO_2 nanoparticles 33% of the dye still remained in the solution. In addition, 53% of the photocatalytic activity of TGH remained after 5 cycles of photocatalytic reaction. In this context, Liu et al. [129] synthesized TiO_2/rGO composite aerogels with con- trollable and continuously tunable surface wettability ranging from super-hydrophilic to super-hydrophobic. The contact angle of the as-prepared TiO_2/rGO aerogels varied from 0° with TiO_2 wt% at 96.7-157° with TiO_2 wt% at 14.5. It was demonstrated that these aerogels show significantly different photocatalytic performances in an aqueous solution containing both lipophilic oleic acid and water soluble MO (Fig. 14). While hydrophobic TiO_2/rGO aerogels adsorbed and degraded oleic acid under irradiation, there was very little activity for MO degradation (Fig. 14a-b). On the other hand, hydrophilicTiO_2/rGO aerogels only degraded MO (Fig. 14c-d), thus showing a better activity than pure P25. This sort of selectivity can be especially useful in systems containing extremely poisonous contaminants in low concentration together with large quantity of non-poisonous chemicals.

Although considerable progress has been achieved, there is room for further research regarding pollution transformation by 3- D graphene/CNT systems. For example, Rao et al. [130] synthesized composites of TiO2 nanoparticles with pure graphene as well as boron- and nitrogen-doped graphene, and studied the photodegra-dation of MB and RhB. The authors showed that MB which is a good electron donor and has a low ionization energy interacts strongly with electron deficient boron-doped graphene resulting in fast degradation of the dye. In addition, RhB which is not a good electron donor and possesses a higher ionization energy, interacts strongly with electron-rich nitrogen-doped graphene, causing a faster degradation of the dye. Such photocatalytic studies on 3- D boron and nitrogen-doped graphene and CNT networks are still scarce and should be further investigated.

Green energy applications

Different energy producing applications can be benefitted through the introduction of 3-D carbon networks, due to their exceptional properties. These new energy producing techniques benefit the environment as they have the potential to decrease the amount of greenhouse gases being released into the atmosphere by the burning of coal.

Energy harvested from water has always been considered as a desirable approach to fulfill the need to energy, from hydropower generation to fuel cells. The electrolysis of water to produce usable H_2 and O_2 could be a clever strategy to provide clean fuel without any environmentally harmful side products. During water splitting, two half reactions happen, which are the hydrogen evolution reac- tion (HER) to produce hydrogen in the cathode, and anode reaction-oxygen evolution reaction (OER) to produce oxygen. An efficient catalyst is needed to drive the reaction with lower input energy,

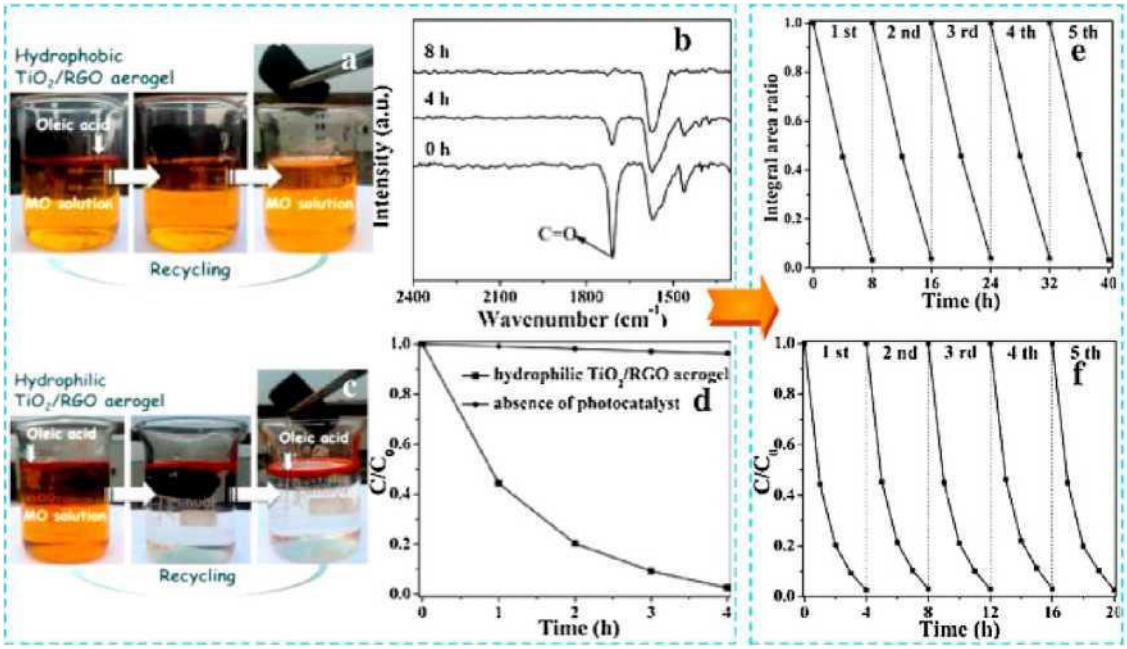

Fig. 14. Photographs showing adsorption and degradation of oleic acid and MO over (a) hydrophobic and (c) hydrophilic rGO/TiO2 aerogels. (b) Comparison of the FT-IR spectra of oleic acid overthe hydrophobic rGO/TiO2 aerogels with respect to time. (d)Temporal changes ofMO concentration overhydrophilic rGO/TiO2 aerogels as monitored by UV-vis spectra. Cycling runs under irradiation of (e) hydrophobic and (f) hydrophilic rGO/TiO2 aerogels [129]. Reprinted with permission from reference 129. Copyright 2015 Elsevier.

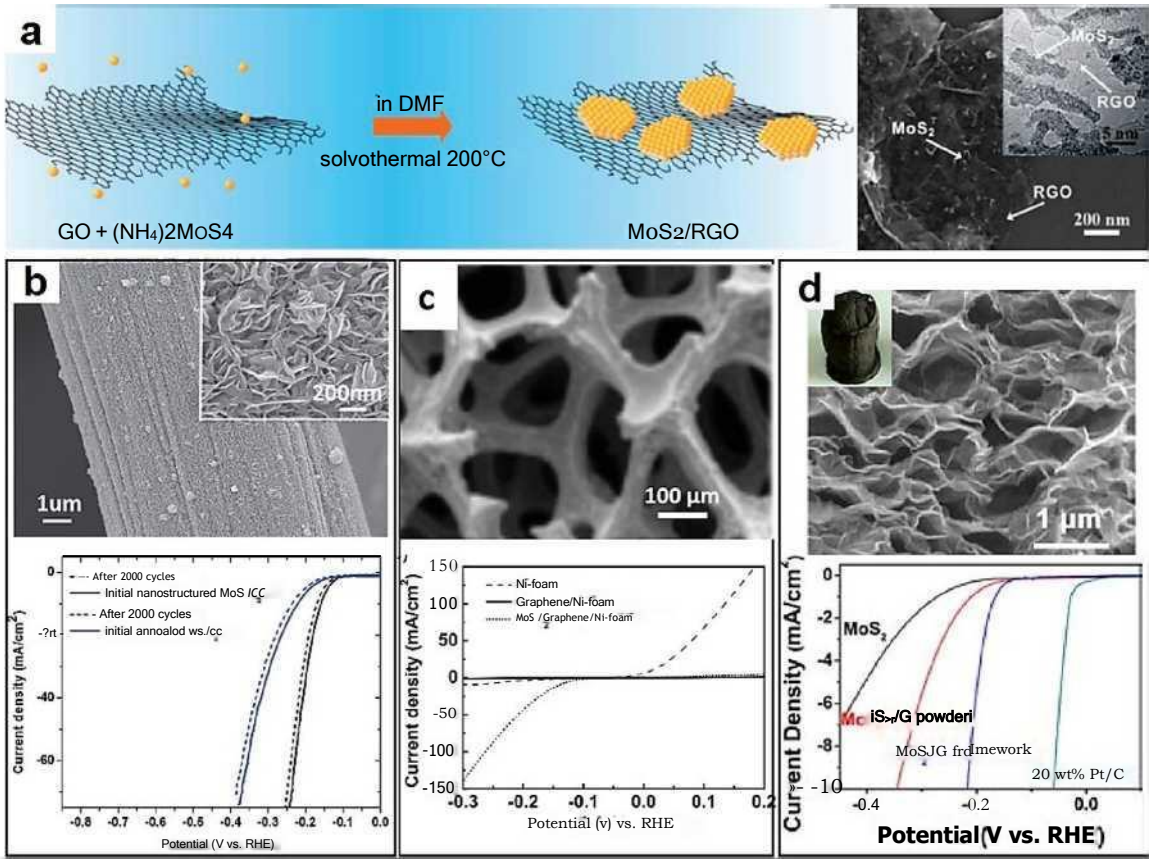

Fig. 15. (a) Schematic synthesis of rGOwith MoS2 bysolvothermal approach, and SEM,TEM images ofthe hybrid structure[140]. *Reprinted with permission from reference 142. Copyright2011 American Chemical Society;* (b)Vertically oriented MoS2 nanosheets on carbon cloth; (above) low and high magnification (inset) SEM images of nanostructured MoS2/C; (below) polarization curves of the electrode before and after 2000 CV scans [141]. *Reprinted with permission from reference 141. Copyright 2014 Royal Society of Chemistry;* (c) MoSx grown on graphene protected Ni foams; (above) SEM image of the 3-D foam with graphene and MoSx; (below) polarization curves [142]. *Reprinted with permission from reference 142. Copyright 2012 John Wiley and Sons;* (d) 3-D hierarchical frameworks ofMoS2 on GO; (above) SEM images of the 3-D framework; (below) polarization curves [143]. *Reprinted with permission from reference 143. Copyright2014 American Chemical Society.*

which means the reduction of overpotential for water Splitting [131]. So far, the HER/OER catalyst with the lowest overpotential, almost to 0 V, is Pt [132]. However, it is well known that its high cost and scarcity could make such clean energy unaffordable. Thus, the discovery and development of an economical and effi- cient catalyst able to replace Pt is imperative [133]. In this regard, myriad materials including metal composites, alloys, and compounds have been explored and studied by electrochemists [134]. Recently 2-dimensional (2D) atomic thin transition metal dichalco- genides (TMDs), such as molybdenum disulfide (MoS_2), have been both theoretically and experimentally confirmed to demonstrate promising activity as a HER catalyst [135], after being ignored for their poor activity in the bulk form [136]. Theoretically, using DFT calculations, the free energy of H adsorption on MoS2, especially Mo-edges (0.08 eV), is closer to Pt [137]. Experimentally, it has been reported that vertically aligned MoS_2 and $MoSe_2$ layers with abundant exposed edges can split the water with a Tafel slope ranging from 75 to 120mV/dec [138]. Also, the 1T phase of MoS_2, which is metallic, exhibits significant HER activity, showing a decreased Tafel slope around 40 mV/dec compared to the 2H phase (semicon- ducting phase) [139]. However, 2H MoS_2 is the room temperature stable phase and not the 1T phase; the stability of the catalyst made by the 1T phase limits its performance. Thus, the combina- tion ofTMDs with conducting carbon materials seems to be a viable approach to increase the conductivity, and accelerate the electronic transport [140]. In 2011, Dai's group reported that by synthesizing MoS_2 directly on rGO sheets (Fig. 15a), here an excellent electri- cal coupling to the underlying graphene sheets contributes to an efficient HER electrode [140]. It is important to note that in 2D carbon materials, perforated structures with more exposed edges and surfaces always result in decreased electrical conductivities. Therefore, systems composed of3-D structured carbon would be an alternative framework to construct robust and effective HER elec- trodes, containing abundant exposed surfaces and edges, as well as an effective 3-D electrical transport network.

Within the vast range of carbon materials, various 3-D struc- tured frameworks have been selected to construct hybrid systems with exposed edges, conducting electrodes and TMDs. For exam- ple, vertically aligned MoS_2 and WS_2 nanosheets can be anchored to a 3-D carbon cloth by a solvothermal method (Fig. 15b), and the polarization curves indicate prominent stability [141].The strong bonding between the TMDs layers and the carbon fiber, along with hydrophobicity, promotes self-removal of the as-formed H2 bubbles. In addition to this, the maximally exposed active edge-sites from the vertically aligned sheets result in a high performance and stable HER catalyst [141]. Another 3-D high surface area and conducting graphene framework is synthesized by chemi- cal vapor deposition (CVD) using Ni foam as a template [144]. In this approach, high quality covalently interconnected graphene sheets result in an outstanding electrical conductivity. Further- more, the addition of MoSx makes these materials HER active (Fig. 15c), giving a Tafel slope as small as 42.8 mV/dec [142]. Other 3-D carbon frameworks, such as rGO sponges (Fig. 15d) [143] and carbon nanofibers [145], also show attractive HER reactivity due to the robust and electrically conductinng characteristics. Regard- ing doping, our group has been investigating (experimentally and theoretically) how the incorporation of W in MoS2/rGO hybrid structures enhances the HER activity due to the increased number of defects sites and a lower H energy barrier. Not only can doping on TMDs enhance the catalytic performance, but also doping of 3-D carbon itself can give rise to novel catalytic properties. For example, it has been reported by Wu et al. that N-doped 3D graphene foams can selectively catalyze CO_2 reduction to CO with long durability at low over-potentials [146].

Solar energy has the potential to be one of the most effective, and clean replacement for current energy sources. Dye-sensitized solar cells (DSSC) are a relatively new alternative for conventional solar cells.They offer competitive traits such as low cost, easy fabrication, and high conversion efficiency. The platinum counter electrode, currently used in DSSCs, is very expensive and efforts to replace it for a more economical materials are underway. In this context, carbon nanostructures have recently been considered for this role due to their many exceptional properties, such as: high conduc- tivity, catalytic activity, easy synthesis, corrosion resistant, and very low cost. However, CNTs powders lack of cohesive mechanical strength and agglomeration stability [147]. Therefore, 3-D carbon nanostructures solve these issues, thus making them much more favorable for this application. In this context, Chen et al. measured conversion efficiency in carbon nanotube foams of up to 6.21% (compared to a measured 7.63% of platinum) [147]. Great electrical conductivity and mechanical strength within the nanotubes caused the high efficiency, especially their ability to stay attached to the substrate [147]. In addition, Ma et al. noted that well-dispersed CNTs perform better than agglomerated CNTs [148]. In order to reduce the agglomeration, the authors used dispersed CNTs with GO sheets, forming a "brick-like" graphene/CNT composite. After nitrogen-doping, the graphene within this "brick" results in con- version efficiencies of 6.74% (compared to 6.89% of platinum) [148]. These composites remained efficient over many cycles owing to their mechanical stability and catalytic reactivity. In this compos- ite, the graphene sheets provided much of the catalytic activity, while the dispersed CNTs help proving the high electrical conduc- tivity. The nitrogen doping of the graphene added to the catalytic activity of the sample, increased the measured efficiency [148]. Therefore, it is clear that 3-D carbon scaffolds will be extremely useful in the development of metal-free hybrid systems that are environmentally friendly and could eventually replace current catalysts. However, further investigations and synthetic alternatives are needed in the near future.

Conclusions and perspectives

Within a short period graphene (2-D) and CNTs (1-D) have evolved into 3-D macroscopic solids, thus bridging their nanoscale properties to materials with novel environmental applications (pollution management). However, there are many opportunities and challenges regarding the synthesis ofthese structures that need to be addressed. More versatile and environment friendly synthesis strategies need to be developed to scale up the production of graphene- and CNT-based sponges. In this regard, the improvement of CVD techniques concerning furnace size and design is important. For GO-based sponges, a fast and scalable method for mass produc- tion of GO from the exfoliation of graphite is yet to be achieved. The GO synthesis is currently limited to the use of concentrated acids, variation of size and functionalities of the produced graphene sheets and the time consuming separation methods. In the near future, improved characterization methods need to be developed to fully understand the surface chemistry of GO and to implement it for improved interactions of GO sheets to form stable 3-D networks. Another challenge consists of gaining precise control of the assembly of the individual building blocks to form periodic 3-D networks. Apart from scalability, most of the sponges discussed through this review are fragile and need careful handling. Thus, further improvements in the robustness of these solid materials is needed. As far as environmental applications are concerned, very little information is available regarding exposure risks for both ani- mals and human beings as well as long term environmental risks of these carbon solids. Even for their nanoscale building blocks e.g. CNTs and graphene, systematic studies are still required to deter- mine, for example, how these materials enter cells, where they are internalized, which cytotoxic mechanisms are relevant and how the

toxicity can be correlated to their physicochemical properties such as size, shape, surface wettability, functionality, doping etc. Biodistribution and nanotoxicity of CNTs- and graphene-based materials should also be tested. Among other issues, engineering of smart porous membranes with these structures for water and gas purification is still at its initial stage. Moving forward, further research and innovation are necessary to harness the properties of novel 3-D graphene/CNT networks for practical applications. We believe that more in-depth studies regarding doped carbon nanostructures and their composites with novel 2-D materials beyond graphene, are needed and will eventually result in real yet futuristic 3-D solids with unprecedented properties.

Acknowledgements

The authors acknowledge the support from US Air Force Office of Scientific Research MURI grant 3A78-15-441 and FA9550-12-1-0471. The authors also acknowledge the support from the National Science Foundation EFRI-Nanopores project # 1542707.

References

[1] R. Tamura, M. Tsukada, Phys. Rev. B. 55 (1997) 4991.
[2] M. Menon, D. Srivastava, Phys. Rev. Lett. 79 (1997) 4453.
[3] J.M. Romo-Herrera, M. Terrones, H. Terrones, S. Dag, V. Meunier, Nano Lett. 7 (2007) 570.
[4] M. Terrones, F. Banhart, N. Grobert, J.-C. Charlier, H. Terrones, P.M. Ajayan, Phys. Rev. Lett. 89 (2002 075505.
[5] M. Endo, H. Muramatsu, T. Hayashi, Y.-A. Kim, G.V. Lier, J.-C. Charlier, et al., Nano Lett. 5 (2005) 1099.
[6] G.K. Dimitrakakis, E. Tylianakis, G.E. Froudakis, Nano Lett. 8 (2008) 3166.
[7] W. Koh, J.I. Choi, S.G. Lee, W.R. Lee, S.S.Jang, Carbon 49 (2011) 286.
[8] S. Nardecchia, D. Carriazo, M.L. Ferrer, M.C. Gutierrez, F. del Monte, Chem. Soc. Rev. 42(2012) 794.
[9] Y. Shen, Q. Fang, B. Chen, Environ. Sci. Technol. 49 (2015) 67.
[10] V. Chabot, D. Higgins, A. Yu, X. Xiao, Z. Chen, J. Zhang, Energy Environ. Sci. 7 (2014) 1564.
[11] W.S. Hummers, R.E. Offeman, J. Am. Chem. Soc. 80 (1958) 1339.
[12] R. Cruz-Silva, A. Morelos-Gomez, H. Kim, H. Jang, F. Tristan, S. Vega-Diaz, et al., ACS Nano 8 (2014) 5959.
[13] H. Bai, C. Li, X. Wang, G. Shi, Chem. Commun. 46 (2010) 2376.
[14] H. Bai, C. Li,X. Wang, G. Shi, J. Phys. Chem. C 115 (2011) 5545.
[15] Y. Xu, Q. Wu, Y. Sun, H. Bai, G. Shi, ACS Nano 4 (2010) 7358.
[16] O.C. Compton, Z. An, K.W. Putz, B.J. Hong, B.G. Hauser, L. Catherine Brinson, et al., Carbon 50 (2012) 3399.
[17] Y. Xu, K. Sheng, C. Li, G. Shi, ACS Nano 4 (2010) 4324.
[18] Y. Wu, N. Yi, L. Huang, T. Zhang, S. Fang, H. Chang, et al., Nat. Commun. 6 (2015) 6141.
[19] X. Zhang, Z. Sui, B. Xu, S. Yue, Y. Luo, W. Zhan, J. Mater. Chem. 21 (2011) 6494.
[20] Z. Niu, J. Chen, H.H. Hng, J. Ma, X. Chen, Adv. Mater. 24 (2012) 4144.
[21] J. Li, J. Li, H. Meng, S. Xie, B. Zhang, L. Li, et al., J. Mater. Chem. A 2 (2014) 2934.
[22] L. Estevez, A. Kelarakis, Q. Gong, E.H. Da'as, E.P. Giannelis, J. Am. Chem. Soc. 133(2011)6122.
[23] C. Li, L. Qiu, B. Zhang, D. Li, C.-Y. Liu, Adv. Mater. 28 (2016) 1510.
[24] L. Qiu, J.Z. Liu, S.L.Y. Chang, Y. Wu, D. Li, Nat. Commun. 3 (2012) 1241.
[25] Z. Wang, Z. Tang, Z. Han, S. Shen, B. Zhao, J. Yang, RSC Adv. 5 (2015) 19838.
[26] R.R. Kohlmeyer, M. Lor,J. Deng, H. Liu, J. Chen, Carbon 49 (2011) 2352.
[27] Y. Li, J. Chen, L. Huang, C. Li, J.-D. Hong, G. Shi, Adv. Mater. 26 (2014) 4789.
[28] T. Liu, M. Huang, X. Li, C. Wang, C.-X. Gui, Z.-Z. Yu, Carbon 100 (2016) 456.
[29] B. Yao, J. Chen, L. Huang, Q. Zhou, G. Shi, Adv. Mater. 28 (2016) 1623.
[30] Z. Xu, C. Gao, ACS Nano 5 (2011) 2908.
[31] H. Sun, L. Cao, L. Lu, Energy Environ. Sci. 5 (2012) 6206.
[32] Z. Chen, W. Ren, L. Gao, B. Liu, S. Pei, H.-M. Cheng, Nat. Mater. 10 (2011) 424.
[33] W.Jiang, H. Xin, W. Li, Mater. Lett. 162 (2016) 105.
[34] M. Xiao, T. Kong, W. Wang, Q.Song, D. Zhang, Q.Ma, et al., Adv. Funct. Mater. 25(2015)6165.
[35] Y. Ito, Y. Tanabe, H.-J. Qiu, K. Sugawara, S. Heguri, N.H. Tu, Angew. Chem. 126 (2014) 4922.
[36] J.-L. Shi, C. Tang, H.-J. Peng, L. Zhu, X.-B. Cheng, J.-Q. Huang, Small 11 (2015) 5243.
[37] X. Du, H.-Y. Liu, Y.-W. Mai, ACS Nano 10 (2016) 453.
[38] A. Morelos-Gomez, P.G. Mani-Gonzalez, A.E. Aliev, E. Munoz-Sandoval, A. Herrera-Gomez, A.A. Zakhidov, et al., Adv. Funct. Mater. 24 (2014) 2612.
[39] B.G. Choi, M. Yang, W.H. Hong, J.W. Choi, Y.S. Huh, ACS Nano 6 (2012) 4020.
[40] K. Chen, C. Li, Z. Chen, L. Shi, S. Reddy, H. Meng, Nano Res. 9 (2016) 249.
[41] Y. Li, J. Wang, X. Tian, L. Ma, C. Dai, C. Yang, et al., Nanoscale 8 (2016) 1676.
[42] F. Dabir, R. Sarraf-Mamoory, M. Loeblein, S.H. Tsang, E.H.T. Teo, Mater. Des. 90(2016)524.
[43] Y.-H. Chang, C.-T. Lin, T.-Y. Chen, C.-L. Hsu, Y.-H. Lee, W. Zhang, et al., Adv. Mater. 25 (2013) 756.
[44] W. Zhou, K. Zhou, D. Hou, X. Liu, G. Li, Y. Sang, et al., ACS Appl. Mater. Interfaces 6 (2014) 21534.
[45] D.P. Hashim, N.T. Narayanan, J.M. Romo-Herrera, D.A. Cullen, M.G. Hahm, P. Lezzi, et al., Sci. Rep. 2 (2012), http://dx.doi.org/10.1038/srep00363.
[46] J.M. Romo-Herrera, B.G. Sumpter, D.A. Cullen, H. Terrones, E. Cruz-Silva, D.J. Smith, et al., Angew. Chem. Int. Ed. 47 (2008) 2948.
[47] Y. Fu, B. Carlberg, N. Lindahl, N. Lindvall, J. Bielecki, A. Matic, et al., Adv. Mater. 24(2012) 1576.
[48] C. Shan, W. Zhao, X.L. Lu, D.J. O'Brien, Y. Li, Z. Cao, et al., Nano Lett. 13 (2013) 5514-5520.
[49] X. Gui, J. Wei, K. Wang, A. Cao, H. Zhu, Y.Jia, et al., Adv. Mater. 22 (2010) 617.
[50] A. Mikhalchan, Z. Fan, T.Q. Tran, P. Liu, V.B.C. Tan, T.-E. Tay, et al., Carbon 102 (2016) 409.
[51] Z. Jin, X. Li, W. Zhou, Z. Han, Y. Zhang, Y. Li, Chem. Phys. Lett. 432 (2006) 177.
[52] I. Ivanov, A. Puretzky, G. Eres, H. Wang, Z. Pan, H. Cui, et al., Appl. Phys. Lett. 89(2006) 223110.
[53] L. Ci, J. Suhr, V. Pushparaj, X. Zhang, P.M. Ajayan, Nano Lett. 8 (2008) 2762.
[54] M.A. Worsley, S.O. Kucheyev, J.H.S. Jr, A.V. Hamza, T.F. Baumann, Appl. Phys. Lett. 94(2009) 073115.
[55] J. Zou, J. Liu, A.S. Karakoti, A. Kumar, D. Joung, Q. Li, et al., ACS Nano 4 (2010) 7293.
[56] S. Roy, A. Banerjee, RSC Adv. 2 (2012) 2105.
[57] L. Lascialfari, C. Vinattieri, G. Ghini, L. Luconi, D. Berti, M. Mannini, et al., Soft Matter 7 (2011) 10660.
[58] J. Chen, C. Xue, R. Ramasubramaniam, H. Liu, Carbon 44 (2006) 2142.
[59] M.B. Bryning, D.E. Milkie, M.F. Islam, L.A. Hough, J.M. Kikkawa, A.G. Yodh, Adv. Mater. 19(2007)661.
[60] K.H. Kim, Y. Oh, M.F. Islam, Adv. Funct. Mater. 23 (2013) 377.
[61] R. Carter, L. Oakes, A.P. Cohn, J. Holzgrafe, H.F. Zarick, S. Chatterjee, et al., J. Phys. Chem. C 118 (2014) 20137.
[62] M. Zhang, B. Gao, X. Cao, L. Yang, RSC Adv. 3 (2013) 21099.
[63] V.C. Tung, L.-M. Chen, M.J. Allen, J.K. Wassei, K. Nelson, R.B. Kaner, et al., Nano Lett. 9 (2009) 1949.
[64] X. Dong, J. Chen, Y. Ma, J. Wang, M.B. Chan-Park, X. Liu, et al., Chem. Commun. 48 (2012) 10660.
[65] L. Ai, J. Jiang, Chem. Eng. J. 192(2012) 156.
[66] H. Sun, Z. Xu, C. Gao, Adv. Mater. 25 (2013) 2554.
[67] H. Hu, Z. Zhao, Y. Gogotsi, J. Qiu, Environ. Sci. Technol. Lett. 1 (2014) 214.
[68] S. Kabiri, D.N.H. Tran, T. Altalhi, D. Losic, Carbon 80 (2014) 523.
[69] K. Goh, W.Jiang, H.E. Karahan, S. Zhai, L. Wei, D. Yu, et al., Adv. Funct. Mater. 25 (2015) 7348.
[70] F. Tristan-Lopez, A. Morelos-Gomez, S.M. Vega-Diaz, M.L. Garcla-Betancourt, N. Perea-Lopez, A.L. Ellas, et al., ACS Nano 7 (2013) 10788.
[71] X. Gan, R. Lv, J. Bai, Z. Zhang, J. Wei, Z.-H. Huang, et al., 2D Mater. 2 (2015) 034003.
[72] X. Gui, A. Cao, J. Wei, H. Li, Y. Jia, Z. Li, et al., ACS Nano 4 (2010) 2320.
[73] A. Marmur, Langmuir 19 (2003) 8343.
[74] M.A. Worsley, P.J. Pauzauskie, T.Y. Olson, J. Biener,J.H. Satcher, T.F. Baumann, J. Am. Chem. Soc. 132 (2010) 14067.
[75] F. Meng, X. Zhang, B. Xu, S. Yue, H. Guo, Y. Luo, J. Mater. Chem. 21 (2011) 18537.
[76] T. Maiyalagan, X. Dong, P. Chen, X. Wang, J. Mater. Chem. 22 (2012) 5286.
[77] Z. Dai, L. Liu, X. Qi, J. Kuang, Y. Wei, H. Zhu, et al., Sci. Rep. 6 (2016) 18930.
[78] K.H. Kim, Y. Oh, M.F. Islam, Nat. Nanotechnol. 7 (2012) 562.
[79] D.C. Miller, M. Terrones, H. Terrones, Carbon 96 (2016) 1191.
[80] A.H. Schoen, Infinite periodic minimal surfaces without self-intersections, Tech Report; NASATechn. Note (1970) D 5541.
[81] Z.-Y. Wu, C. Li, H.-W. Liang, Y.-N. Zhang, X. Wang, J.-F. Chen, et al., Sci. Rep. 4 (2014), http://dx.doi.org/10.1038/srep04079.
[82] L. Li, G. Zhou, Z. Weng, X.-Y. Shan, F. Li, H.-M. Cheng, Carbon 67 (2014) 500.
[83] M.S. Mauter, M. Elimelech, Environ. Sci. Technol. 42 (2008) 5843.
[84] B. Yu, J. Xu,J.-H. Liu, S.-T. Yang,J. Luo, Q. Zhou, et al., J. Environ. Chem. Eng. 1 (2013) 1044.
[85] V. Janout, S.B. Myers, R.A. Register, S.L. Regen, J. Am. Chem. Soc. 129 (2007) 5756.
[86] A.M. Atta, R.A.M. El-Ghazawy, R.K. Farag, A.-A.A. Abdel-Azim, J. Polym. Res. 13 (2006) 257.
[87] M. Inagaki, A. Kawahara, H. Konno, Carbon 40 (2002) 105.
[88] T. Ono, T. Sugimoto, S. Shinkai, K. Sada, Nat. Mater. 6 (2007) 429.
[89] T. Ono, T. Sugimoto, S. Shinkai, K. Sada, Adv. Funct. Mater. 18 (2008) 3936.
[90] Y. Chu, Q. Pan, ACS Appl. Mater. Interfaces 4 (2012) 2420.
[91] J. Yuan, X. Liu, O. Akbulut, J. Hu, S.L. Suib, J. Kong, et al., Nat. Nanotechnol. 3 (2008) 332.
[92] A. Sayari, S. Hamoudi, Y. Yang, Chem. Mater. 17 (2005) 212.
[93] C. Wu, X. Huang, X. Wu, R. Qian, P. Jiang, Adv. Mater. 25 (2013) 5658.
[94] H. Bi, X. Xie, K. Yin, Y. Zhou, S. Wan, L. He, et al., Adv. Funct. Mater. 22 (2012) 4421.
[95] M. Toyoda, M. Inagaki, Carbon 38 (2000) 199.
[96] Y. Qian, I.M. Ismail, A. Stein, Carbon 68 (2014) 221.
[97] Y. Zhao, C. Hu, Y. Hu, H. Cheng, G. Shi, L. Qu, et al., Angew. Chem. Int. Ed. 51 (2012) 11371.
[98] H. Li, L. Liu, F. Yang, J. Mater. Chem. A 1 (2013) 3446.
[99] C. Cheng, S. Li, J. Zhao, X. Li, Z. Liu, L. Ma, et al., Chem. Eng. J. 228 (2013) 468.

[100] C. (Sage) Cheng,J. Deng, B. Lei,A. He,X. Zhang, L. Ma, et al.,J. Hazard. Mater. 263(2013)467.
[101] Z.-Y. Sui, Y. Cui,J.-H. Zhu, B.-H. Han, ACS Appl. Mater. Interfaces 5 (2013) 9172.
[102] O. Barbier, G.Jacquillet, M. Tauc, M. Cougnon, P. Poujeol, Nephron Physiol. 99 (2005) 105.
[103] S.J. Grayston, S. Wang, C.D. Campbell, A.C. Edwards, Soil Biol. Biochem. 30 (1998)369.
[104] H. Gao, Y. Sun,J. Zhou, R. Xu, H. Duan, ACS Appl. Mater. Interfaces 5 (2013) 425.
[105] Y. Lei, F. Chen, Y. Luo, L. Zhang, Chem. Phys. Lett. 593 (2014) 122.
[106] X. Mi, G. Huang, W. Xie, W. Wang, Y. Liu,J. Gao, Carbon 50 (2012) 4856.
[107] G. Zhao, X. Ren, X. Gao, X. Tan,J. Li, C. Chen, et al., Dalton Trans. 40 (2011) 10945.
[108] C.C. Mancheng,J. Liu, Phys. Chem. C115 (2011), http://dx.doi.org/10.1021/jp208575m.
[109] N. Zhang, H. Qui, Y. Si, W. Wang, J. Gao, Carbon 49 (2011) 827.
[110] R. Li, Q. Li, S. Gao, J.K. Shang,J. Am. Ceram. Soc. 94 (2011)584.
[111] J. Wang, X. Li, J.S. Ince, Z. Yue,J. Economy, Sep. Sci. Technol. 45 (2010) 1058.
[112] J. Liu, X. Ge, X. Ye, G. Wang, H. Zhang, H. Zhou, et al., J. Mater. Chem. A 4 (2016) 1970.
[113] Y. He, N. Zhang, F. Wu, F. Xu Y. Liu,J. Gao, Mater. Res. Bull. 48 (2013) 3553.
[114] P.M. Sudeep, T.N. Narayanan, A. Ganesan, M.M. Shaijumon, H. Yang, S. Ozden, et al., ACS Nano 7 (2013) 7034.
[115] J. Liang, Z. Cai, L. Li, L. Guo, J. Geng, RSC Adv. 4 (2014) 4843.
[116] F. Yavari, Z. Chen, A.V. Thomas, W. Ren, H.-M. Cheng, N. Koratkar, Sci. Rep. 1 (2011).
[117] M.R.J. Scherer, Double-Gyroid-Struct Funct. Mater., SpringerInternational Publishing, 2013, pp. 135-156.
[118] J.J. Miasik, A. Hooper, P.T. Moseley, B.C. Tofield, Conducting Polymers, SpringerNetherlands Publishing, 1987, pp. 189-198.
[119] T. Alizadeh, F. Ahmadian, Anal. Chim. Acta 897 (2015) 87.
[120] X. Feng, W. Chen, L. Yan, Sens. Actuators B Chem. 215 (2015) 316.
[121] Y.-H. Zhang, Y.-B. Chen, K.-G. Zhou, C.-H. Liu, J. Zeng, H.-L. Zhang, et al., Nanotechnology 20 (2009) 185504.
[122] Y. Long, C. Zhang, X. Wang,J. Gao, W. Wang, Y. Liu, J. Mater. Chem. 21 (2011) 13934.
[123] H. Huang, P. Chen, X. Zhang, Y. Lu, W. Zhan, Small 9 (2013) 1397.
[124] Y. Zhang, Y. Liu, X. Wang, Z. Sun,J. Ma, T. Wu, et al., Carbohydr. Polym. 101 (2014) 392.
[125] B.Adhikari,A. Biswas,A. Banerjee,ACS Appl. Mater. Interfaces 4 (2012) 5472.
[126] Z. Zhang, F. Xiao, Y. Guo, S. Wang, Y. Liu, ACS Appl. Mater. Interfaces 5 (2013) 2227.
[127] N.H. Le, H. Seema, K.C. Kemp, N.Ahmed,J.N.Tiwari, S. Park, et al., J. Mater. Chem. A 1 (2013) 12900.
[128] T. Wu, M. Chen, L. Zhang, X. Xu, Y. Liu,J. Yan, et al., J. Mater. Chem. A 1 (2013) 7612.
[129] W. Liu, J. Cai, Z. Ding, Z. Li, Appl. Catal. B Environ. 174-175 (2015) 421.
[130] K. Gopalakrishnan, H.M. Joshi, P. Kumar, L.S. Panchakarla, C.N.R. Rao, Chem. Phys. Lett. 511 (2011)304.
[131] J. Xie, Y. Xie, ChemCatChem 7 (2015) 2568.
[132] M.H. Miles, J. Electroanal. Chem. Interfacial Electrochem. 60 (1975) 89.
[133] W. Sheng, H.A. Gasteiger, Y. Shao-Horn,J. Electrochem. Soc. 157(2010) B1529.
[134] M.G. Walter, E.L. Warren,J.R. McKone, S.W. Boettcher, Q. Mi, E.A. Santori, et al., Chem. Rev. 110 (2010) 6446.
[135] C. Tan, H. Zhang, Chem. Soc. Rev. 44 (2015) 2713.
[136] H. Tributsch, J. Bennett, J. Electroanal. Chem. 81 (1977) 97.
[137] M.V. Bollinger, K.W.Jacobsen,J.K. NOrskov, Phys. Rev. B 67 (2003) 085410.
[138] D. Kong, H. Wang,J.J. Cha, M. Pasta, K.J. Koski,J. Yao, et al., Nano Lett. 13 (2013) 1341.
[139] D. Voiry, M. Salehi, R. Silva, T. Fujita, M. Chen, T. Asefa, et al., Nano Lett. 13 (2013)6222.
[140] Y. Li, H. Wang, L. Xie, Y. Liang, G. Hong, H. Dai, et al., J. Am. Chem. Soc. 133 (2011)7296.
[141] Y. Yan, B.Xia, N. Li, Z. Xu, A. Fisher,X.Wang,J. Mater. Chem.A3(2015) 131.
[142] Y.-H. Chang, C.-T. Lin, T.-Y. Chen, C.-L. Hsu, Y.-H. Lee, et al., Adv. Mater. 25 (2013) 756.
[143] W. Zhou, K. Zhou, D. Hou, X. Liu, G. Li, Y. Sang, et al., ACS Appl. Mater. Interfaces 6 (2014) 21534.
[144] Z. Chen, W. Ren, L. Gao, B. Liu, S. Pei, H.-M. Cheng, Nat. Mater. 10(2011)424.
[145] X. Guo, G. Cao, F. Ding, X. Li, S. Zhen, Y. Xue, et al., J. Mater. Chem. A 3 (2015) 5041.
[146] J. Wu, M. Liu, P.P. Sharma, R.M. Yadav, L. Ma, Y. Yang, et al., Nano Lett. 16 (2015) 466.
[147] J. Chen, F. Meng, X. Gui, Carbon 50 (2012) 5624.
[148] C. J. Ma, F. Li, J. Chen Yu, J. Power Sources 273 (2015) 1048.

Archi Dasgupta received her Bachelors in Chemistry from Presidency College, University of Calcutta, India. She graduated with a M.S. degree from Solid State and Structural Chemistry Unit, Indian Institute of Science, Bangalore, India in 2011. She is currently working towards her PhD degree in Chemistry under the supervision of Prof. Mauricio Terrones at the Pennsylvania State University, USA. Archi's research interest includes synthesis of three dimensional networks of CNTs, surface physical and chemical characterization of graphitic nanomaterials as well as studying theiradsorptive properties towards environmental pollutants.

Lakshmy Pulickal Rajukumar completed her B.Tech in Metallurgical and materials engineering from National Institute of Technology, Tiruchirappalli, India, in 2011. She recently received her PhD degree in Materials Science and Engineering under the supervision of Prof.Mauricio Terrones at the Pennsylvania State University, USA. Lakshmy's research focus includes synthesis and characterization of novel nanomaterials, particularly doped carbon nanotubes (CNTs), 3-D networks of CNTs, graphene-CNT hybrids as well as CVD synthesis ofTMDs.

Christopher Rotella received his Bachelors of Science in Physics from Rowan University, USA. He is currentlywork- ingtowards his Ph.D. in Materials Science and Engineering under Prof. Mauricio Terrones at The Pennsylvania State University, USA.H is research is focused on creatingthree- dimensional carbon nano-structures through different growth and post-growth techniques.

Yu Lei graduated with a B.S. and M.S degree in material science and engineering from TsinghuaUniversity, China, in 2011 and 2013, respectively. She is currently pursuing a PH.D. in Material Science and Engineering underthe guidance ofProf. Mauricio Terrones at the Pennsylvania State University, USA. Her research interests are 2 dimensional materials including graphene and transition metal dichacholgenide, and their energy conversion applications.

Mauricio Terrones is Professor of Physics, Chemistry, and Materials Science & Engineering at the Pennsylvania State University. He is also the founding Director of the Centerfor 2-Dimensional and Layered Materials at Penn State since March 2013. He is a renowned scientist in carbon nanomaterials including CNTs and graphene; and other layered nanomaterials e.g. nitrides, and chalcogenides. He has co-authored more than 400 publications in leading journals including *Nature, Science, Nature Materials, Nature Nanotechnology, Nature Chemistry, Nature Communications, Physical Review Letters, ACS, Nano, Nano Letters, Advanced Materials*, etc. His work has been cited more than 35,000 times and his H index is 85 (Google Scholar 96). Mauricio obtained his doctorate degree with Sir Prof. Harold W. Kroto (Nobel Laureate, FRS) from The University of Sussex in 1998. He has been recipient of the Mexican National Prize for Chemistry, theJaved Husain Prize, Albert Einstein medal from UNESCO, the TWAS Prize in Engineering Physics, and others. He is member of the Mexican Academy of Sciences, TWAS fellow, fellow of the American Association for the Advancement of Science (AAAS), fellow of the Royal Society of Chemistry, UK.H e is the principal editor of *Carbon*, *Journal of Materials Research, 2D Materials* and *Materials Express*.